Available online at www.sciencedirect.com
SCIENCE DIRECT®
PERGAMON
Polyhedron 22 (2003) 2963–2983
POLYHEDRON
www.elsevier.com/locate/poly

Oligopyrrole-based solid state self-assemblies

Jonathan L. Sessler [a,*], Guillaume Berthon-Gelloz [a], Philip A. Gale [b,*], Salvatore Camiolo [b], Eric V. Anslyn [a], Pavel Anzenbacher Jr. [a], Hiroyuki Furuta [c], Gregory J. Kirkovits [a], Vincent M. Lynch [a], Hiromitsu Maeda [c], Pierfrancesco Morosini [a], Markus Scherer [a], Jim Shriver [a], Rebecca S. Zimmerman [a]

[a] *Department of Chemistry and Biochemistry, 1 University Station – A5300, The University of Texas at Austin, Austin, TX 78712-1167, USA*
[b] *Department of Chemistry, University of Southampton, Southampton SO17 1BJ, UK*
[c] *Department of Chemistry & Biochemistry, Graduate School of Engineering, Kyushu University, Fukuoka 812-8581, Japan*

Received 20 August 2002; accepted 28 February 2003

Abstract

The ability of pyrrole-containing species to form higher order self-assembled ensembles and aggregates in the solid state is reviewed. The different binding modes pyrrole adopts in stabilizing these systems are analyzed as are the various underlying hydrogen bonding interactions upon which they are predicated.

Keywords: Supramolecular chemistry; Self-assemblies; Solid state structures; Pyrroles; Hydrogen bonds; Molecular recognition

1. Introduction

Hydrogen bond-mediated self-assembly represents an area of considerable current interest. Represented by a broad spectrum of approaches it is giving rise to an ever increasing level of activity [1–10]. Its relevance towards biological systems is undeniable and research in this area is clearly critical to efforts to understand the grand scheme of Nature's design. In this context, it is apparent that, the study of simple structural motifs that undergo hydrogen bond-mediated self-assembly can help us understand the subtle mechanisms involved in the formation of biological "superstructures", including those associated with nucleic acid oligomers, multi-component enzymes, cell membranes, and viral capsids, to name but a few [11–13].

Our initial entry into this particular sub-branch of supramolecular chemistry came through the study of pyrrole-based entities bearing appended anionic entities and the finding that these systems would dimerize both in the solid state and in relatively apolar solvents [14]. More recently, we and others have come to appreciate that neutral pyrrolic entities are also capable of undergoing self-assembly especially in the solid state [15–18]. In this paper, we review the underlying chemistry associated with the latter class of hydrogen bond-predicated ensembles, presenting both published and unpublished results that help illustrate the diversity of structural motifs that may be stabilized in the solid state.

2. Common binding motifs in pyrrole-based self-assemblies

As will be detailed in the course of the discussion, there are several common binding motifs that underlie the formation of most self-assembled structures in which pyrrole plays a critical role. Therefore, prior to analyzing on a case-by-case basis, individual ensembles, it is perhaps instructive to summarize in general terms the key features of these motifs. Probably, the most recurrent binding motif is that represented by Structure **I** in

* Corresponding authors. Tel.: +1-512-471-5009; fax: +1-512-471-7550 (J.L. Sessler), Tel.: +44-23-80593332; fax: +44-23-80596805 (P.A. Gale).
E-mail addresses: sessler@mail.utexas.edu (J.L. Sessler), Philip.gale@soton.ac.uk (P.A. Gale).

0277-5387/$ - see front matter © 2003 Elsevier Ltd. All rights reserved.
doi:10.1016/S0277-5387(03)00436-4

Scheme 1; it arises commonly when a pyrrole is substituted on the α (or 2) position by a carbonyl-containing functional group (e.g., aldehyde, ketone, ester, and amide) or an appropriate analogue (e.g., imine); this substitution pattern often leads to dimerization of two such entities, wherein the H-bond donor (the pyrrolic N*H*) and acceptor (carbonyl or carbonyl-like moiety) are adjacent to one another. The net result is a structure that bears similarity to classic Watson–Crick nucleotide base-pairs. Throughout this review, this most common of binding modes will be referred to as the "classic" binding mode.

Although possessing a carbonyl subunit, and thus capable of supporting a "classic" binding mode (Structure **I**; Scheme 1), amides can also act as hydrogen bond donors by virtue of their NH functionality. Rotation around the C2(pyrrole)—CONH bond thus gives a convergent binding site represented by Structure **IIa** in Scheme 2. This latter structural motif is less common than the "classic" one but is of greater interest as far as the complexation of anions is concerned.

In broadening the scope of these common motifs, one can classify the different motifs of pyrrole-based self-assemblies into three categories. The first one is based on pyrroles substituted in the 2 position; such subunits display dual behavior in the solid state, either forming discrete dimers (Structure **IIIa**; Scheme 3) or infinite hydrogen bonded networks characterized by "head-to-tail" arrangements (Structure **IIIb**; Scheme 3).

A second key self-assembly motif, very similar to the first, occurs when pyrroles are substituted in the 3 position. In this case, at least as far as we have been able to note, the pyrrole unit appears unable to dimerize. Thus, only a "head-to-tail" arrangement is observed (Structure **IV**; Scheme 4).

The third and final general self-assembly situation involves what can be considered in general terms as "third party-mediated" hydrogen bonded networks. Here, typically a solvent molecule (e.g., water, dichloromethane, dimethoxyethane, etc.) or an anion (e.g., acetate, fluoride chloride, etc.) serves as the hydrogen bond acceptor (Structure **V**; Scheme 5).

Using one or a combination of these basic self-assembly motifs, one can construct an unlimited number of more complex self-assemblies. One simple example is the formation of molecular ribbons by linking together two dimerized units (Structure **VI**; Scheme 6). Representative

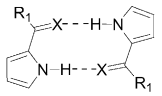

I

X= O, N

R_1= H, Alkyl, Ph, OR, NHR

Scheme 1. "Classic" binding mode adopted by pyrrolic compounds bearing a carbonyl group in the 2 or 5 positions.

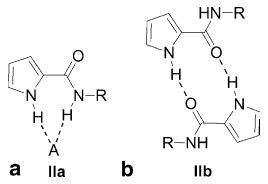

Scheme 2. Illustration of inherent duality in binding that is possible for pyrrole amide derivatives. (a) Convergent binding mode and (b) "classic" binding mode. The charges on the species "A", if any, have been omitted.

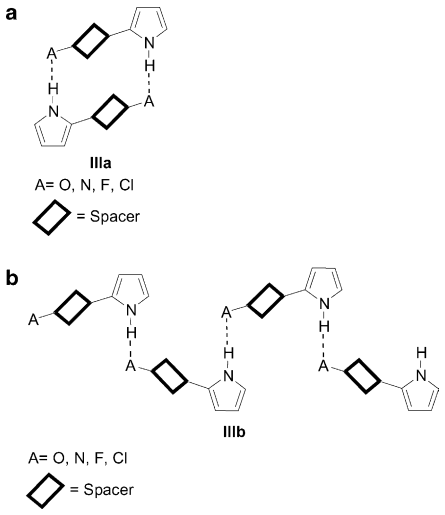

Scheme 3. Representation of the two most prevalent types of self-assembly observed in the case of pyrroles bearing substituents in the 2 or 5 positions. (a) Dimerization and (b) "head-to-tail" supramolecular network formation. The charges on the species "A", if any, have been omitted.

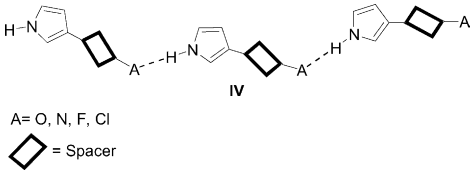

Scheme 4. "Head-to-tail" hydrogen bonded network observed in the case of many 3-substituted pyrroles.

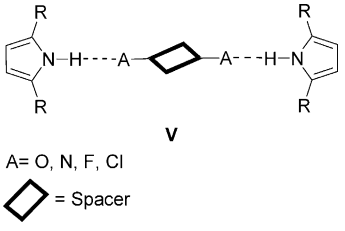

Scheme 5. Illustration of pyrrole-containing self-assembled ensembles stabilized by ancillary or "third party" species (e.g., solvent, counter anion, etc.). The charges on the species "A", if any, have been omitted.

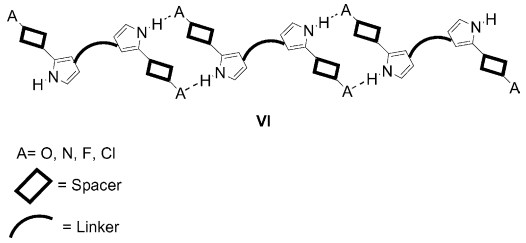

Scheme 6. Schematic representation of supramolecular ribbon structures resulting from hydrogen bond interactions involving individual dimer subunits. The charges on the species "A", if any, have been omitted.

examples of this and other motifs will now be presented in the context of specific chemical structures.

3. Charged entities

3.1. Macrocyclic oligopyrroles

As indicated above, our entry into the area of pyrrole-based ensemble construction came about as the result of preparing carboxyl-functionalized, "tailed" polypyrrole macrocycles. The first such system was the doubly substituted sapphyrin (**1**) [14]. Under normal conditions, this species exists as a zwitterion, something that is not surprising when account is taken of the acidic Nature of the carboxyl group and the high intrinsic basicity of free-base, neutral sapphyrins; compound **1** is thus best considered as consisting of a protonated sapphyrin "head" and an appended carboxylate anion "tail". Given the known propensity of protonated sapphyrins to act as anion receptors, it was expected that compound would self-associate in some fashion. Initial evidence for self-assembly, particularly in the gas phase, came from low- and high-resolution fast atom bombardment mass spectrometry. Solution phase ^{1}H NMR spectroscopic analyses, carried out in methanol-d_4/$CDCl_3$ (2/1) mixture and vapor pressure osmometry (VPO) studies, carried out in 1,2-dichloroethane, led to the conclusion that the dominant form of this interaction was in terms of a self-assembled dimer. Such dimer formation, supported the initial assessment, made using CPK models, that length of the tail precluded a narcissistic interaction, wherein the protonated sapphyrin "head" wrapped around to "bite" its own "tail" (Fig. 1). Interestingly, but not unexpectedly, addition of fluoride anion, an anionic species bound by sapphyrins far more strongly than carboxylate anions, served to break up the dimer [19].

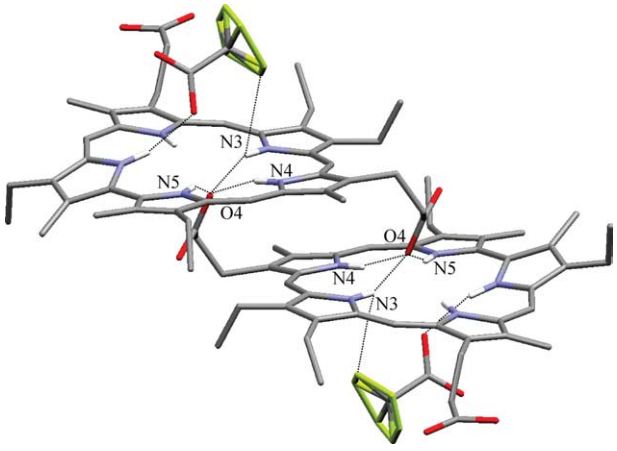

Fig. 1. Side view of the supramolecular sapphyrin dimer **1**·**1**. The macrocycles are related by a crystallographic inversion center at 1/2, 1/2, 0. The vertical separation between the root mean square (RMS) planes of the nitrogen atoms of each macrocycle in this structure is 3.39(1) Å. This figure was generated using information downloaded from the Cambridge Crystallographic Data Centre and corresponds to a structure reported in [14]. Atom color codes in: red, oxygen; blue, nitrogen; gray, carbon; and green, fluoride.

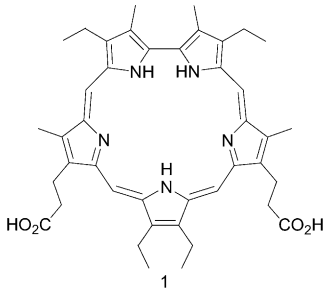

1

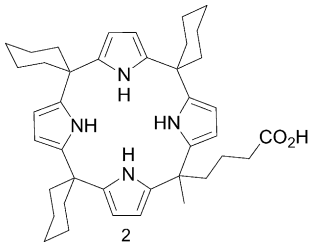

2

Solid state structural studies supported the structural inferences drawn from the solution phase analyses and revealed specifically that in the solid state, the carboxylate tail is anchored to a neighboring protonated sapphyrin core through three hydrogen-bonds. Although the hydrogen-bond angles (N_3—H···O_4 = 150.51(12)°, N_4—H···O_4 = 160.4(12)°, and N_4—H···O_4 = 157.7(11)°) are severely distorted from the ideal value of 180°, their lengths, 2.763(13), 2.816(13), and 2.81(14) Å, for $d_{N_3O_4}$, $d_{N_4O_4}$, $d_{N_5O_4}$, respectively, are quite short, implying a strong electrostatic interaction with the charged sapphyrin core. The vertical separation between the root mean square (RMS) planes of the nitrogen atoms of the two macrocycles in this dimer is 3.39(1) Å. This separation is manifested in the context of a beautifully aligned dimer wherein the individual sapphyrin subunits are related to

one another by a crystallographic inversion center at 1/2, 1/2, 0.

The linked "head" and "tail" strategy was further developed in the context of the neutral anion receptor calix[4]pyrrole [20]. Here, a carboxylate "tail" was attached to a calix[4]pyrrole via one of the meso-like bridging positions forming the functionalized species **2** (Fig. 2). While solution phase studies revealed only incomplete self-assembly in methanol, solid state structural analyses revealed exactly the same type of dimer seen in the case of sapphyrin (**1**), except that the vertical separation between the RMS planes of the nitrogen atoms in the individual macrocycles in the dimer is 7.41(1) Å. Each of the individual calix[4]pyrroles within the dimer **2**·**2** adopts a cone conformation, as is the norm for anion complexes of related systems [20]. This conformation allows the formation of four hydrogen-bonds to the corresponding carboxylate tail.

In the solid state, the hydrogen bonds formed between the carboxylate tail and the four nitrogens of the calix[4]pyrrole in dimer **2**·**2** have average lengths of 2.955 Å for the critical N(pyrrole)···O(ester) tethering interaction. The average N(pyrrole)—H···O(ester) angle in **2** is 167°. This angle is much closer to the ideal than that seen in the solid state structure of dimer **1**·**1**. Although, four hydrogen bonding interactions are seen in dimer **2**·**2**, as opposed to three seen in **1**·**1**, the lengths of these bonds are on average longer by 0.16 Å than in the case of the sapphyrin dimer (average N(pyrrole)···O(ester) distance = 2.796 Å). Presumably, this reflects a reduced level of electrostatic interaction in the case of the neutral calix[4]pyrrole receptors.

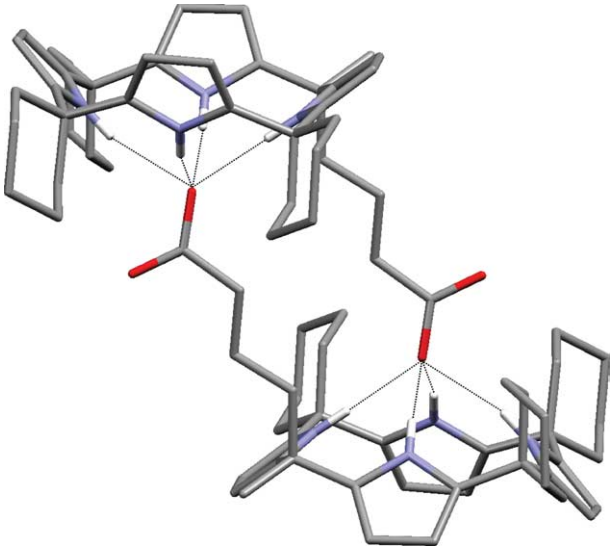

Fig. 2. Side view of the noncovalent calix[4]pyrrole dimer **2**·**2**. The vertical separation between the root mean square (RMS) planes of the nitrogen atoms in this structure is 7.41(1) Å. This figure was generated using information downloaded from the Cambridge Crystallographic Data Centre and corresponds to a structure reported in [14]. Atom color codes in: red, oxygen; blue, nitrogen; and gray, carbon.

In these systems, the information needed to form a self-assembled dimer is "built in" to the molecule through the judicious choice of polypyrrolic "head", spacer, and carboxylate "tails". The net result is something that can be viewed as an information storage system, where the formation or non-formation of a given type of dimerized structural motif represents one bit of information.

3.2. Simple pyrrole entities

Recently, Schmuck et al. [21–23] have introduced a new type of building block that consists of a charged guanidiniocarbonyl pyrrole. Originally designed for the selective recognition of anions through the introduction of various hydrogen bond donors, these simple entities have been found to form self-assembled structures in the solid state. The first guanidiniocarbonyl pyrrole reported by these workers, compound **3**, forms an interesting acetate-mediated ensemble in the solid state (Fig. 3).

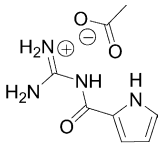

3

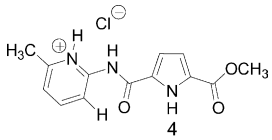

4

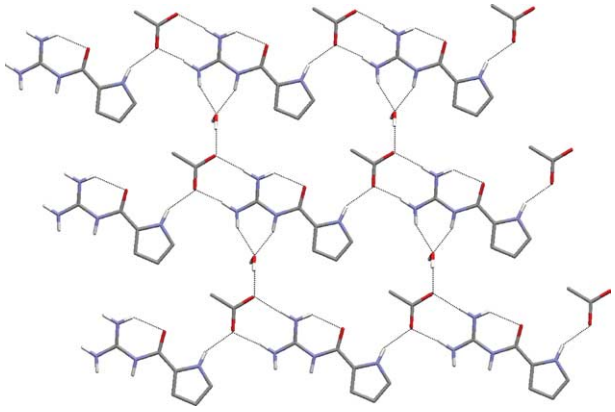

Fig. 3. View of the crystal structure of **3** highlighting the extended two dimensional, planar network formed by the solid state self-assembly of the guanidiniocarbonyl pyrrole acetate (**3**). This figure was generated using information downloaded from the Cambridge Crystallographic Data Centre and corresponds to a structure reported in [22]. Atom color codes in: red, oxygen; blue, nitrogen; and gray, carbon.

The acetate anion is embedded within what is an extended two-dimensional hydrogen bonding network. Electrostatic interactions involving the cationic guanidinium moiety and the acetate are thus presumably the predominant structure-defining forces. Consistent with this, the guanidinium NH protons are found to bind the complexed acetate anions in a bidentate H-bonding fashion as known for simple guanidinium salts [24,25]. These hydrogen bonds are highly stable as seen by the very short N(guanidinium)···O(acetate) distance of 2.801 Å. The additional hydrogen bond provided by a pyrrole unit from an adjacent receptor molecule likely provides further stabilization for the overall supramolecular structure. The relevant N(pyrrole)—O(acetate) distance is 2.89 Å; however, the N(pyrrole)H···O(acetate) angle is 145°, a value that is clearly suboptimal.

Schmuck et al. have also explored the self-assembly of an amide-pyridinium functionalized pyrrole unit wherein C—H···O hydrogen bonds are observed. These latter interactions are of interest because they can stabilize motifs that are isostructural to ones derived from pyrrole N—H···O hydrogen bonds. This type of interaction was specifically found in dimer **4**·**4** (Fig. 4). In this structure, the two pyrrolic subunits are held together by a long N(pyrrole)—H···O(amide) hydrogen bond, giving an N(pyrrole)—O(amide) distance of 3.166 Å. These weak hydrogen bonds are complemented by two C—H···O interactions involving the pyridinium C3—H and the carboxyl CO. The C···O distance is 2.946 Å and the C—H···O angle is 135.5°. These distances are surprisingly short since generally the C···O distance in analogous systems is greater than 3 Å. The C—H···O bond angle of 135° is rather small, but C—H···O hydrogen bonds are more flexible than N—H···O hydrogen bonds. In this event, taken in concert, these observations are consistent with the C—H···O interactions playing an important role in stabilizing the overall ensemble.

4. Neutral entities

4.1. Amide pyrrole systems

Perhaps the first amide pyrrole assemblies recognized as such came about in the context of preparing a bipyrrole-based [2]catenane [26]. One of the offshoots of this work, designed to produce a new kind of topographically nonplanar anion receptor, was the synthesis of a bipyrrole-5,5′-di(benzylamide) (**5**). This species was successfully characterized by X-ray diffraction analysis (Fig. 5). The resulting structure helped to make clear that pyrroles and amides, if suitably linked, can work together to form a convergent binding site that points toward, and interacts with, a hydrogen bond acceptor. Such motifs, represented by Structure **IIa** in Scheme 2, are quite common and can actually, with the benefit of hindsight, be traced back to structures in the literature that antedate that of **5** [26,27].

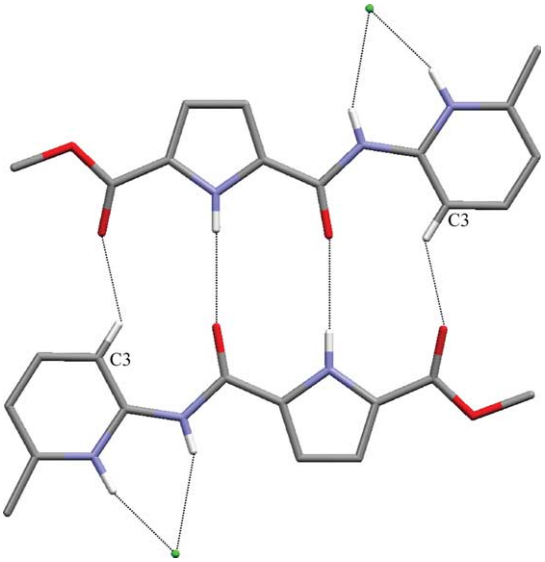

Fig. 4. Crystal structure of dimer **4**·**4**. This figure was generated using information downloaded from the Cambridge Crystallographic Data Centre and corresponds to a structure reported in [23]. Atom color codes in: red, oxygen; blue, nitrogen; gray, carbon; and green, chloride.

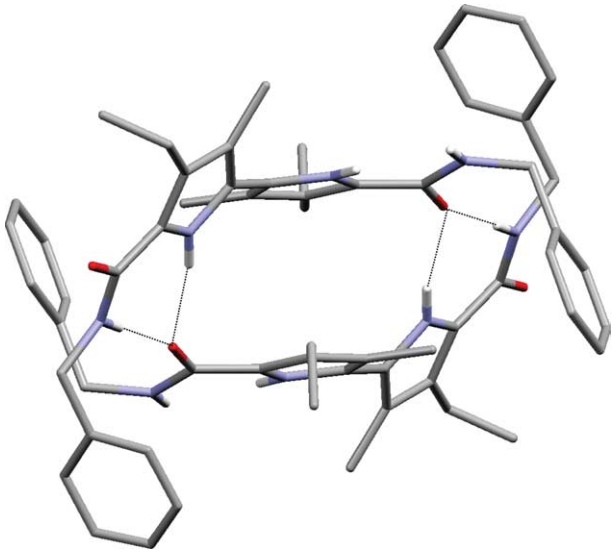

Fig. 5. View of the supramolecular dimer **5**·**5** formed in the solid state by self-assembly of the amide-functionalized bipyrrole units. This dimer is stabilized, among other things, by bifurcated hydrogen bonds involving the amide NH—CO and pyrrolic NH moieties. This figure was generated using information downloaded from the Cambridge Crystallographic Data Centre and corresponds to a structure reported in [26]. Atom color codes in: red, oxygen; blue, nitrogen; and gray, carbon.

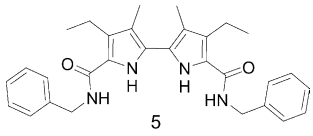

5

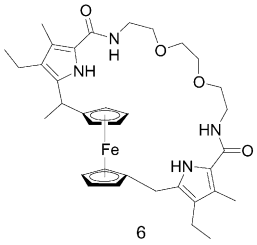

6

In terms of specifics, in the case of **5**, the amide functionalized bipyrrole units form a supramolecular dimer in the solid state, stabilized among other things, by two sets of hydrogen bonds involving the amide NH and the pyrrole NH of one monomeric unit that converge onto the carbonyl hydrogen bond acceptor functionality of the second monomeric unit. This convergent hydrogen bond is asymmetric and shows a shorter NH(pyrrole)···O(amide) separation of 2.816 Å, as compared to the longer NH(amide)···O(amide) distance of 2.861 Å. On the other hand, the NH(amide)—O(amide) angle is more linear than the corresponding NH(pyrrole)—O(amide) angle (171° versus 161°).

The same year the structure of **5** (in the form of its 1:1 dimer, **5**·**5**) was reported, a second solid state X-ray diffraction structure involving the same kind of convergent donor, bifurcating acceptor hydrogen-bonding motif was solved [27]; it was that of the *ansa*-ferrocene (**6**) (Fig. 6). Compound **6** forms an interesting dimer in the solid state, one in which the two subunits come together in a complementary fashion. The resulting convergent hydrogen bond lengths (N(pyrrole)H···O(amide) = 2.999 Å′ and N(pyrrole)H···O(amide) = 3.046 Å) are appreciably longer than the corresponding hydrogen bond lengths seen in dimer **5**·**5** (vide supra). On the other hand, the N(pyrrole)—H···O(amide) and N(amide)—H···O(amide) angles, of 170° and 175°, respectively, are more linear than those found in **5**·**5**.

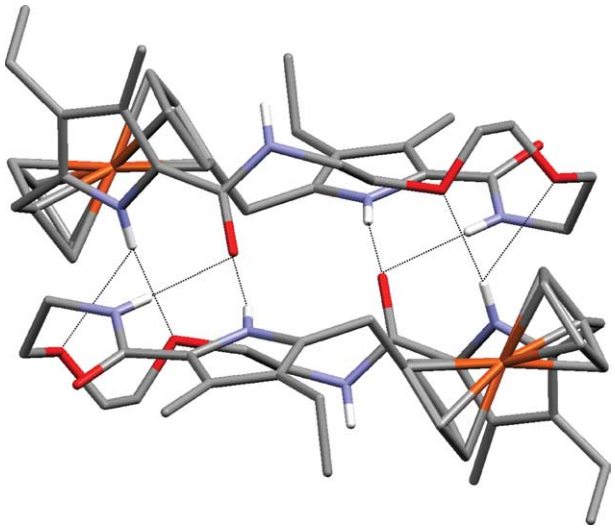

Fig. 6. View of the hydrogen bond-linked dimer **6**·**6** found in the solid state. This figure was generated using information downloaded from the Cambridge Crystallographic Data Centre and corresponds to a structure reported in [27]. Atom color codes in: red, oxygen; blue, nitrogen; gray, carbon; and orange, iron.

4.2. Simple pyrrole units

4.2.1. Pyrrole ferrocene hybrids

For the design of systems with well-defined long-range order (e.g., molecular ribbons and tapes), it was considered advantageous to incorporate at least two pyrrole units within a given monomeric subunit. Here, the specific use of a ferrocene moiety was considered propitious, since the ferrocene unit could both act as a molecular "ball-bearing", giving the system an extra degree of freedom (often useful in stabilizing multicomponent ensembles), and as a redox active marker group [28]. These design considerations led to the preparation of targets **7** and **8** (cf. Figs. 7 and 8) [29].

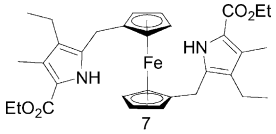

7

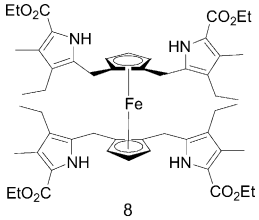

8

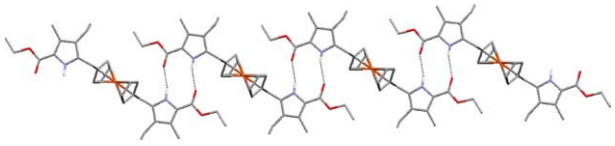

Fig. 7. Side views of the tetrameric subunits contained within the infinite ribbon structures provided by the solid state self-assembly of **7**. This figure was generated using information downloaded from the Cambridge Crystallographic Data Centre and corresponds to a structure reported in [29]. Atom color codes in: red, oxygen; blue, nitrogen; gray, carbon; and orange, iron.

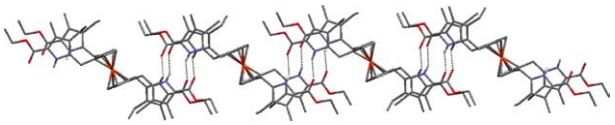

Fig. 8. Side views of representative tetrameric subunits, analogous to those in formed by **7**, found in the infinite ribbon structures formed by **8**. This figure was generated using information downloaded from the Cambridge Crystallographic Data Centre and corresponds to a structure reported in [29]. Atom color codes in: red, oxygen; blue, nitrogen; gray, carbon; and orange, iron.

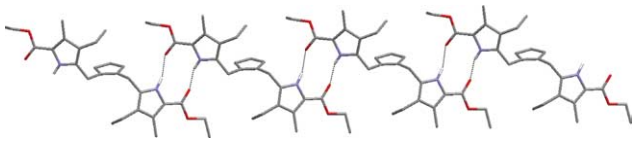

Fig. 9. Side views of representative tetrameric subunits contained within the infinite self-assembled ribbon present in single crystals of **9**. This figure was generated using information downloaded from the Cambridge Crystallographic Data Centre and corresponds to a structure reported in [30]. Atom color codes in: red, oxygen; blue, nitrogen; and gray, carbon.

In both **7** and **8**, the central ferrocene ball-bearing adopts a *trans* geometry, presumably to minimize steric repulsion effects. The solid state structure of **7** further reveals strong intermolecular H-bond interactions between the pyrrolic NH and ester functionalities that result in the formation of infinite ribbons. The intermolecular separation between the pyrrole nitrogens and the ester oxygens was found to be 2.95 Å, while the N—H···O angle was found to be 164°. This latter angle deviates somewhat from the ideal value of 180°, reflecting the need to accommodate the intermolecular hydrogen bond bridges spanning the two noncovalently linked pyrrole units.

In the solid state structure of **8**, similar hydrogen bonding features are found. In this instance, the individual tetrapyrrolic ferrocenes subunits are linked by eight hydrogen bonds. Since this is twice the number of intermolecular contacts found in the ribbons of **7**, this leads to a smaller inter-subunit separation than in this simpler system. Specifically, the N(pyrrole)-to-O(ester) hydrogen bond distance of 2.89 Å seen in the solid structure of **8** is 0.06 Å shorter than seen in the case of **7**. The need in the case of **8** to accommodate a greater number of hydrogen bonds than in **7** leads to a further deviation from linearity in the N—H···O angle (average value = 145° in **8** versus 164° in **7**).

Structures **7** and **8** represent rather unique cases within the fast emerging field of neutral, pyrrole-based self-assembly in that aggregation was established not only in the solid state but also in solution and in the gas phase. One of the molecular attributes that permitted the latter experimental work was the presence of the ferrocene (Fc) moiety. In situ oxidation with I_2 gave the charged Fc^+ species that was particularly easy to study by ESI-MS. Meanwhile, more conventional approaches, involving VPO measurements, carried out in toluene, and ^1H NMR spectroscopy dilution studies in $CDCl_3$ provided support for the contention that **8** exists primarily as a trimer in the solution state but also revealed that **7** is predominantly monomeric under these conditions.

In the course of preparing the tetrapyrrole (**8**), Sessler and co-workers [30] synthesized the bis(pyrrole)cyclopentadiene (**9**) and were able to solve the single crystal X-ray diffraction structure of this intermediate. In the resulting structure of (Fig. 9), hydrogen bonding motifs are seen that are severely ruffled as compared to what is observed in the solid state structures of **7** and **8**.

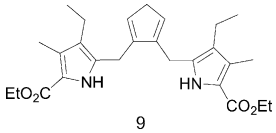

9

For instance in **9**, the torsion angle between the two hydrogen bonded pyrrole ester units, as reflected in the dihedral angle defined by N(pyrrole)1, O(ester)2, N(pyrrole)2, and O(ester)1, is 26.32°; this is much larger than the corresponding values of 0° and 0.86° seen in the solid state structures of **7** and **8**, respectively. The hydrogen bond lengths, in particular the N(pyrrole)—O(ester) distance, is 2.83 Å on average. The average N—H···O angle is 161°. While this represents a deviation from the ideal value of 180°, it represents less of an angular distortion than that seen in the structure of **8**.

4.2.2. Pyrrole amide clefts

Inspired in part by Crabtree's work [31] with amide-based anion receptor "clefts", Gale conceived the idea of developing a molecular cleft containing a pyrrolic unit within the cleft. In a first series of efforts to develop this concept, he and his co-workers [15–18] have prepared a series of receptors based on a 2,5-diamidopyrrole core. These systems, quite apart from their rich and interesting anion binding properties, have led to the characterization of a large number of self-assembled ensembles in the solid state.

The first series of self-assembled systems produced by the Gale group is exemplified by compound **10**. The crystal structure of this compound reveals the formation of both a dimer and a polymer bridged by intramolecular hydrogen bonds (Fig. 10) [17].

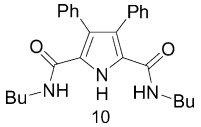

10

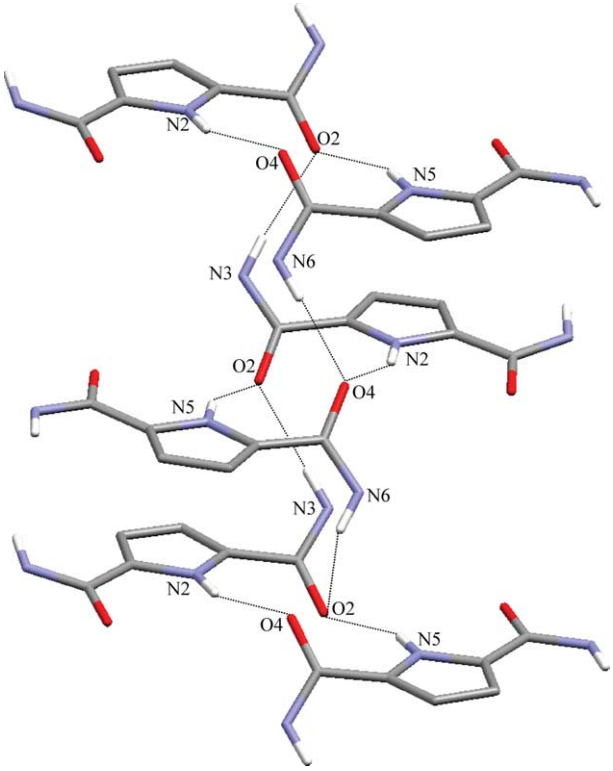

Fig. 10. View of the solid state of **10**. In this structure a dimer is formed via the formation of two hydrogen bonds between the pyrrolic NH and the carbonyl group (average N(pyrrole)···OC distance 2.961(4) Å); a second hydrogen bond is formed between an amide group and the carbonyl group of two discrete dimers (average N(amide)···OC distance 3.021(4) Å), leading to the formation of a polymer that extends along the *c* axis. Phenyl and butyl groups omitted for clarity. This figure was generated using information downloaded from the Cambridge Crystallographic Data Centre and corresponds to a structure reported in [17]. Atom color codes in: red, oxygen; blue, nitrogen; and gray, carbon.

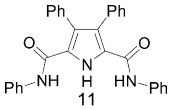

11

In the dimer, the constituent monomers are linked together via two hydrogen bonds involving the pyrrolic NH and the carbonyl group (average N(pyrrole)···O(amide) distance = 2.961(4) Å). The dimers themselves are further organized into chains that extend along the crystallographic *c* axis as the result of hydrogen bonds linking the carbonyl group and the amide NH of two discrete dimeric units (average N(amide)···O(amide) distance = 3.021(4) Å).

Another interesting compound produced by the Gale group is the bis-phenylamide pyrrole (**11**), analogous to **10**. In analogy to what had previously been observed by Schmuck et al. in the case of compound **4** (cf. Section 3.2) [23] compound **11** forms centrosymmetric dimers in the solid state as the result of both intermolecular N—H···O and C—H···O hydrogen bonds (Fig. 11). The

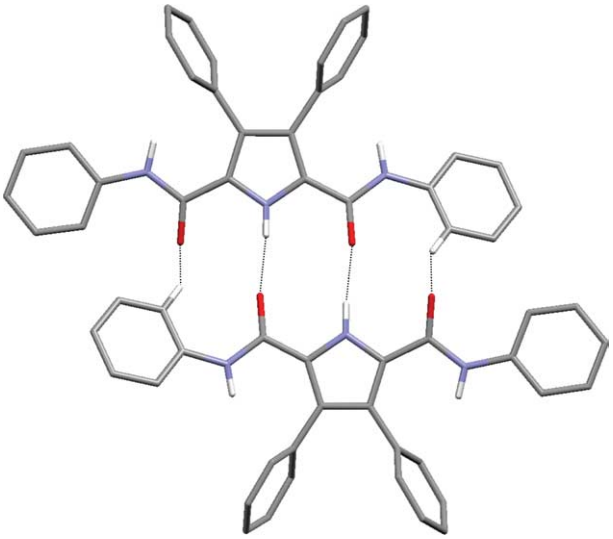

Fig. 11. Crystal structure of **11**. The formation of the dimers **11**·**11** is due to intramolecular hydrogen bonds involving the pyrrolic NH and the carbonyl groups (N(pyrrole)···OC distance = 3.238(4) Å) and the one phenylic CH and the carbonyl (C(phenyl)···OC distance = 3.271(4) Å). This figure was generated using information downloaded from the Cambridge Crystallographic Data Centre and corresponds to a structure reported in [17]. Atom color codes in: red, oxygen; blue, nitrogen; and gray, carbon.

distance between the pyrrolic nitrogen and the carbonyl group is 3.238(4) Å, whereas the length of the C(phenyl)···O(amide) hydrogen bond is 3.271(4) Å.

Several of the control compounds prepared by Gale et al., namely the pyrrole monoamide clefts amide clefts **12** and **13,** bear an even greater resemblance to the functionalized pyrroles characterized structurally by Neidle and co-workers in 1972 [32]. That these venerable systems defined self-assembled aggregates in the solid state was appreciated by the original authors but is underscored by the work of Gale and co-workers. For instance, these latter researchers noted that **12** and **13** formed dimers and, in certain cases, polymers in the solid state [18]. On the other hand, dilution studies (carried out using ^{1}H NMR spectroscopic methods) revealed that such self-association does not occur in DMSO-d_6 solution.

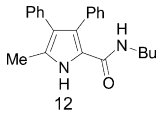

12

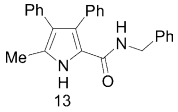

13

Recently, Gale and co-workers [16] have expanded on the basic concepts of amidopyrrole clefts by appending

ferrocenes for the electrochemical detection of anions (producing receptor **14**), ammonium arms (giving rise to **15**) [33], and "crowned" phenyl units **16** [34]. In all cases, the systems in question were seen to dimerize in the solid state via the same binding mode seen in the case of **10** and **11**, namely that illustrated by Structure **I** in Scheme 1.

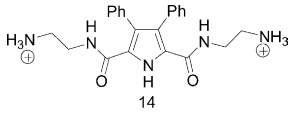

14

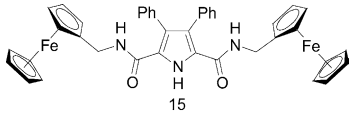

15

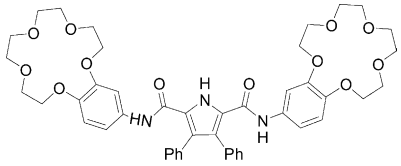

16

Another compound related to **11**, but displaying a very different self-assembly mode, is the nitrophenyl-containing system **17** recently described by Gale and co-workers [35].

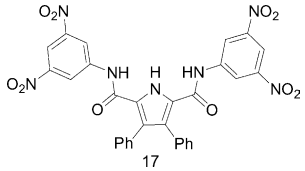

17

In this instance, X-ray diffraction analysis (Fig. 12) reveals that in the solid state an infinite sheet is stabilized via NH···ON(nitro) hydrogen bonds (N···O distance = 3.8967(4) Å). Although the N(pyrrole)—ON(nitro) distance is very long, it is of interest to note that this specific interaction is more favorable, at least in the solid state, than the alternative NH···carbonyl dimer-forming modes that are normally seen in pyrrole amide receptors (cf., e.g., Structure **IIb**, Scheme 2).

4.2.3. A pyrrole diamide cleft bearing chlorine substituents

In an effort to enhance further the anion binding capabilities of pyrrole amide clefts, Gale and co-workers [36] synthesized receptor **18** that contains electron-withdrawing chlorine atoms in the 3 and 4 positions of the pyrrolic ring. This compound is readily deprotonated by a large excess of fluoride, to produce the corresponding anion, [**18**-H$^+$]$^-$.

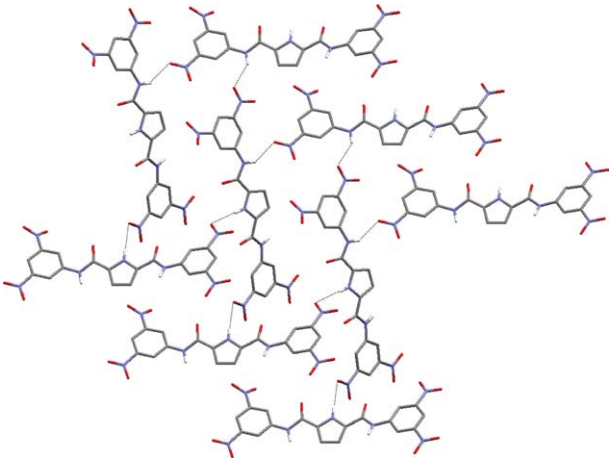

Fig. 12. Solid state structure of compound **17**, a compound analogous to **11** but displaying a very different self-assembled binding mode. Phenyl rings at the 3- and 4-positions of the pyrrole have been omitted for clarity. N(amide)H···ON(nitro) hydrogen bonds mediate the formation of a sheet (N···O distance = 3.8967(4) Å). This figure was generated using information downloaded from the Cambridge Crystallographic Data Centre and corresponds to a structure reported in [35]. Atom color codes in: red, oxygen; blue, nitrogen; and gray, carbon.

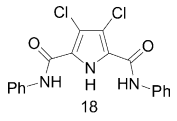

18

A single crystal X-ray diffraction analysis (Fig. 13) revealed no trace of a bound fluoride anion, nor of HF. Rather, a tetrabutylammonium counter cation is seen in the crystal lattice, although it is not proximate to the pyrrole amide receptor. However, these same structural analyses reveal that the deprotonated form of **18** exists as a dimer in the solid state. It is linked as such as the result of four hydrogen bonds that involve the amide NH groups and the anionic pyrrolic nitrogen center. Within the dimer, the individual receptor molecules are found to lie perpendicular to one another, with the amide NH-to-pyrrolic distance being 3.13 Å. Additional π—H interactions between the phenyl hydrogen and the pyrrole ring, with distances on the order of 2.46–2.64 Å, are also observed in the solid state. Presumably, these latter interactions play some ancillary role in stabilizing the observed supramolecular structure. The two amide moieties of each pyrrole are almost co-planar to the pyrrolic ring, deviating from planarity by only 0.98(6)° and 2.36(6)°, respectively.

The finding that the deprotonated form of **18** dimerizes is of interest above and beyond the specific details of the structure. This is because each of the subunits is anionic, meaning that bringing them together is contrathermodynamic in the absence of a significant degree of compensating stabilization. That a well-organized

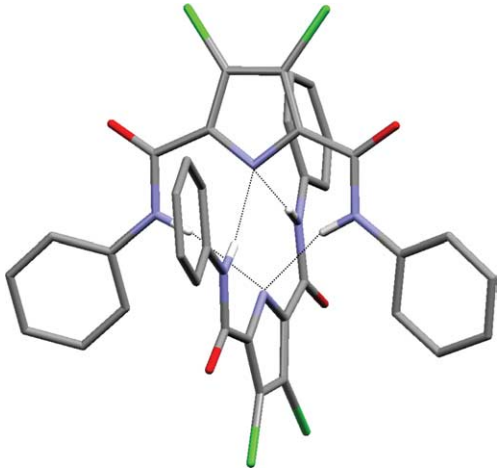

Fig. 13. Solid state structure of [**18**-H$^+$]$^-$. In its deprotonated form, **18** dimerizes in the solid state as the result of four hydrogen bonds between the amide NH groups and the deprotonated pyrrolic nitrogen (distances N(amide)$\cdots$N(pyrrole) = 3.218(4), 3.130(4), 3.124(4), and 3.072(4) Å). The tetrabutylammonium counter cations are not proximate to the dimer and have been omitted for clarity. This figure was generated using information downloaded from the Cambridge Crystallographic Data Centre and corresponds to a structure reported in [36]. Atom color codes in: red, oxygen; blue, nitrogen; and gray, carbon.

structure is formed wherein the counter cation plays no apparent stabilizing role, thus serves to underscore just how strong the noncovalent bonding interactions are.

4.2.4. Ensembles formed as the result of anion–anion self-assembly

Using anionic components to direct the self-assembly of noncovalently linked molecular architectures is a relatively new area of supramolecular chemistry [37–42]. In the context of pyrrole-based ensembles, it has recently been developed successfully by Gale et al. Appreciating that compound **18** undergoes facile deprotonation in the presence of fluoride, they linked synthetically two such individual subunits by a phenyl ring to generate compound **19** (Fig. 14). Deprotonating with excess fluoride anion then produced a species that was found to exist as an interlocked supramolecular polymeric assembly in the solid state [43].

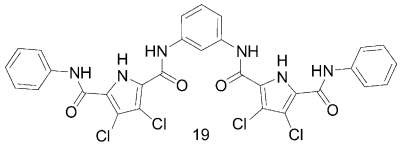

The solid state supramolecular assembly of [**19**-2H$^+$]$^{2-}$ is characterized by hydrogen bonding interactions that are analogous to those seen in [**18**-H$^+$]$^-$. On the other hand, the structure of [**19**-2H$^+$]$^{2-}$ reveals a system with a more highly strained conformation than that present in [**18**-H$^+$]$^-$. This could reflect the fact that

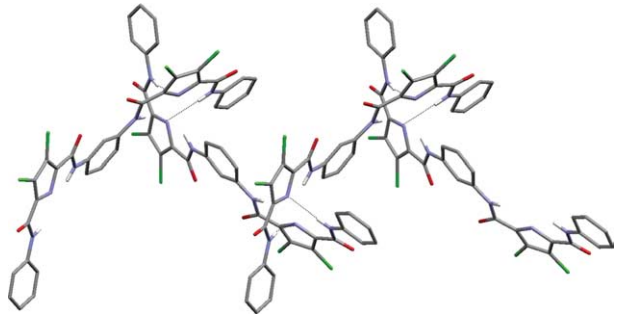

Fig. 14. Solid state structure of the interlocked supramolecular assembly of [**19**-2H$^+$]$^{2-}$, a species generated by the deprotonation of **19** with tetrabutylammonium fluoride. Counter cations have been omitted for clarity. This figure was generated using information downloaded from the Cambridge Crystallographic Data Centre and corresponds to a structure reported in [43]. Atom color codes in: red, oxygen; blue, nitrogen; and gray, carbon.

dimers derived from [**19**-2H$^+$]$^{2-}$ are essentially held together by two hydrogen bonds instead of four, as in the case of [**18**-H$^+$]$^-$. The complementary subunits in dimers [**19**-2H$^+$]$^{2-}$ are disposed in an asymmetrical fashion.

4.2.5. Self-assembly properties of a tren-derived amide-pyrrole tripod

One of the themes that is emerging as the study of pyrrole-based ensembles advances is that relatively simple pyrrole-containing structures can provide complex solid state self-assemblies. Such an impression is underscored in the case of the tris(2-(2-amidepyrrole)ethyl)amine (**20**) (Fig. 15) [44], obtained from the condensation of pyrrole carboxylic acid and tris(2-aminoethyl)amine (tren). This pyrrole amide tripod contains six hydrogen bond donors and three H-bond acceptor sites.

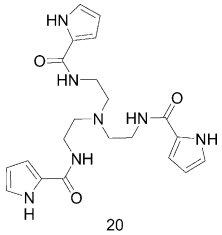

20

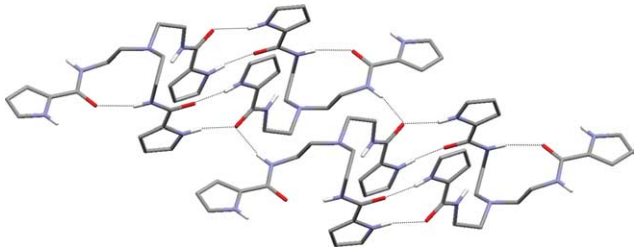

Fig. 15. View of the X-ray structure of tripod **20** showing the extended hydrogen-bonded network present in the solid state. Atom color codes in: red, oxygen; blue, nitrogen; and gray, carbon.

The solid state structure of **20** reveals a self-assembled array wherein one arm is bound in an intramolecular fashion by an N(amide)···O(amide) H-bond (for which an N(amide)···O(amide) distance of 2.897(12) Å was observed), while the two other arms are bound to an adjacent subunit in a "classic" fashion (cf. Structure **I** of Scheme 1). The net result is a dimer held together by four hydrogen-bonds. In this dimer, the average N(pyrrole)···O(amide) distance is 2.811(13) Å, which is relatively short. This dimer is also by itself a subunit or component of an extended "inter-dimer" hydrogen bonded network. The N(pyrrole)···O(amide) spacing between "dimers" within this network, 2.911(13) Å, is 0.1 Å longer than in the dimer itself (for which a N(amide)-O(amide) distance of 2.988(12) Å is observed).

4.3. Oligopyrroles

4.3.1. Bipyrrole

In 1999, Merz et al. synthesized 5,5′-diphenyl-3,3′,4,4′-tetramethoxy-2,2′-bipyrrole (**21**). This species has the intriguing characteristic of crystallizing in two different polymorphic states with a smooth transition between these states taking place at 90 °C [45]. Both forms were analyzed by X-ray diffraction analysis. The resulting solid state structures, **21a** and **21b**, revealed the presence of hydrogen bonding interactions between the pyrrolic hydrogen and the oxygen atoms of the inner methoxy groups.

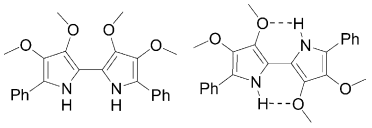

21a 21b

In the solid state, structure **21a** exists in the form of a supramolecular helix whose supramolecular form is maintained by a "head-to-tail" assembly of the individual tretramethoxy bipyrrole subunits (Fig. 16). The *syn* oriented bipyrroles are arranged so as to define turns of 90° along a C2 axis, again reflecting the presence of specific intermolecular hydrogen bonds.

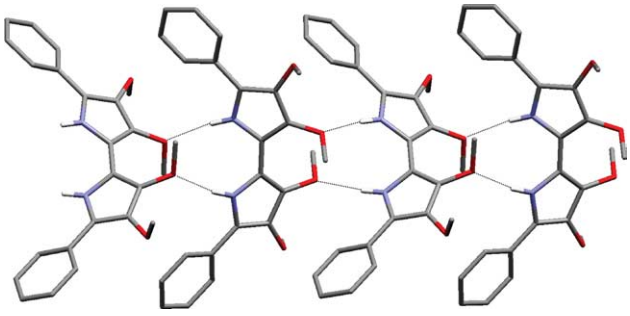

Fig. 16. Supramolecular helix formed by the self-assembly of **21a** as observed in the solid state at low temperatures. This figure was generated using information downloaded from the Cambridge Crystallographic Data Centre and corresponds to a structure reported in [45]. Atom color codes in: red, oxygen; blue, nitrogen; and gray, carbon.

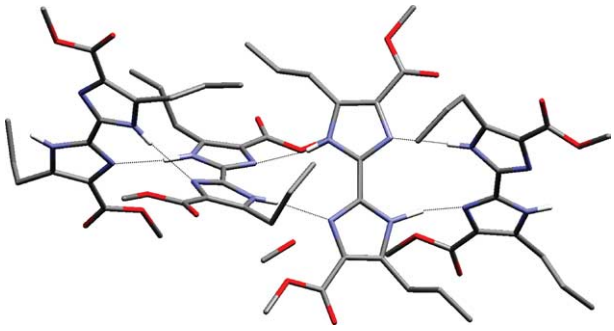

Fig. 17. Molecular structure of biimidazole (**22**) showing the hydrogen bonding interactions between the two nearest neighboring molecules. This figure was generated using information downloaded from the Cambridge Crystallographic Data Centre and corresponds to a structure reported in [46]. Atom color codes in: red, oxygen; blue, nitrogen; and gray, carbon.

The supramolecular helix seen in the case of **21a** is similar to ones observed by Sessler et al. [46] wherein organic-solubilized biimidazoles (**22**) were used as the individual self-assembling subunits (Fig. 17). In the case of the latter biimidazole-derived ensembles, the structural analogy to DNA is more apparent than in the case of **21a** since the helix contains six, rather than four, subunits per 360° helix turn. To the extent to which the analogy to DNA holds, systems such as **21a** and **22** can be considered to be "reversed" or "inverted" analogues of DNA, wherein each subunit can be viewed as being as representing a covalently linked "base pair" [46].

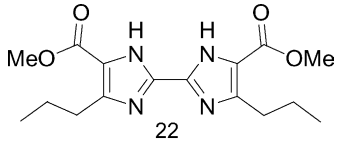

22

In the case of **21**, the initial low temperature polymeric structure defined by **21a** was seen to rearrange to the thermodynamically more stable structure **21b** which is characterized by the presence of intramolecular hydrogen bonds (Fig. 18). The intermolecular hydrogen bonds seen in the solid state structure **21a** are very long (i.e., the N(pyrrole)—O(methoxy) distance is 3.130 Å). By contrast, the intramolecular H-bonds present in **21b** are shorter by 0.22 Å. This could explain why the low temperature species, **21a**, is metastable and readily rearranges to produce **21b** upon heating.

4.3.2. Tris(bipyrrolyl)methane

Tripyrrylmethane enjoyed an early reputation as being notoriously unstable. Its ephemeral nature was reinforced early on when the bacterial pigment prodigiosin (a pyrrolylbipyrrole) was originally, albeit incorrectly,

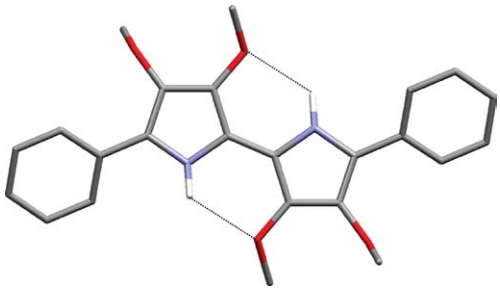

Fig. 18. Solid state structure of **21b**. The pyrrole moieties are stabilized in a nearly planar D_{2h} *anti* conformation as the result of intramolecular hydrogen bonds. This figure was generated using information downloaded from the Cambridge Crystallographic Data Centre and corresponds to a structure reported in [45]. Atom color codes in: red, oxygen; blue, nitrogen; and gray, carbon.

assigned such a structure. Appreciating this fact, Sessler et al. took up the challenge of trying to prepare higher order species based on bipyrrole. These efforts culminated in the preparation of the tris(bipyrrolyl)methane (**23**), a species that they successfully characterized by X-ray diffraction analysis, as well as by ^{1}H NMR spectroscopic means [47].

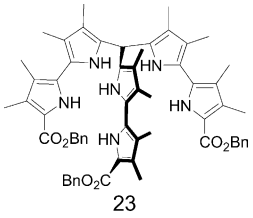

23

In the solid state, compound **23** was found to exist as a hydrogen-bonded dimer (Fig. 19) that was "stitched together" by no fewer than 12 hydrogen bonds involving the individual benzyl ester carbonyl oxygens and the various pyrrolic N—H protons. Each individual carbonyl oxygen atom was found to be within hydrogen bonding distance of two pyrrole rings on an adjacent tripod subunit. One of these contacts involves the carbonyl and one of the outermost pyrroles, while the other involves an interior pyrrole on a neighboring arm of the tripod. The N···O hydrogen bond distances range from 2.85(2) to 3.11(2) Å, while the N—H···O bond angles range from 134(1)° to 159(1)°. The H···O···H angles range from 100.7(6)° to 113.0(6)°. Individual monomers possess either a right- or left-handed twist, with identical twists pertaining to each of the subunits within the dimer. On the other hand, the overall lattice contains an equal number of D and L dimers, meaning no net chirality is observed. Nonetheless, as a result of the hydrogen bonding interactions that lead to dimerization, system **23** defines a kind of supramolecular cryptand, an observation that inspires the suggestion that small guest molecules could be incorporated within its "walls".

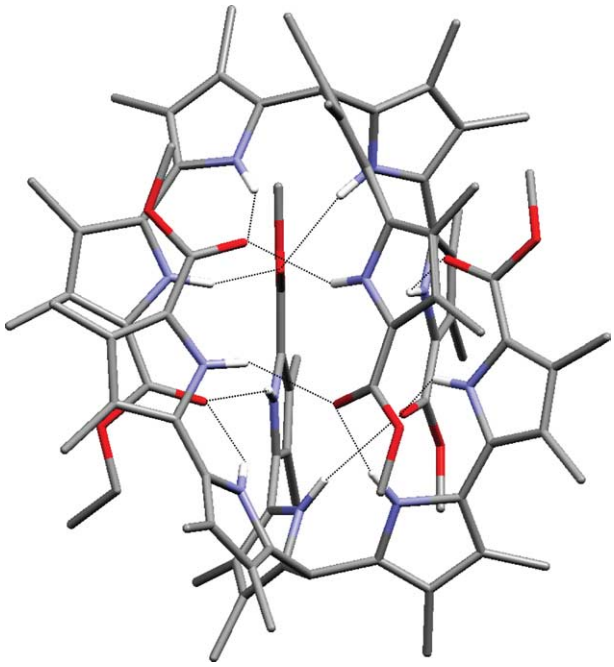

Fig. 19. X-ray structure of the dimer **23**·**23**. Each of the carbonyl oxygen atoms of one molecule is found within hydrogen bonding distance of two pyrrolic NH protons present in a second molecule. Phenyl rings have been omitted for clarity. This figure was generated using information downloaded from the Cambridge Crystallographic Data Centre and corresponds to a structure reported in [47]. Atom color codes in: red, oxygen; blue, nitrogen; and gray, carbon.

4.3.3. Terpyrrole

Terpyrrole has been introduced by Sessler et al. [48] as versatile building block for the synthesis of novel expanded porphyrins. The diethyl ester analogue **24** of this relatively simple molecule forms a hydrogen bonded supramolecular helix in the solid state that highlights the helical twist of the hexaalkyl substituted 2,2′,2″-terpyrrole subunit (Fig. 20).

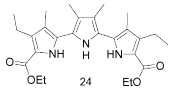

24

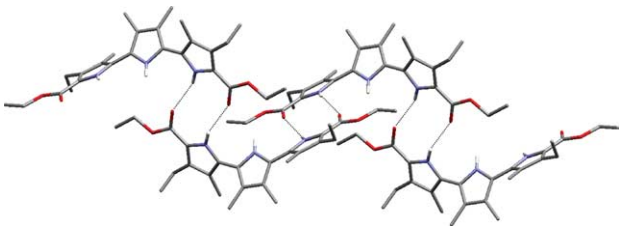

Fig. 20. View of the solid state structure of the supramolecular ensemble produced by the self-assembly of terpyrrole (**24**). This figure was generated using information downloaded from the Cambridge Crystallographic Data Centre and corresponds to a structure reported in [48]. Atom color codes in: red, oxygen; blue, nitrogen; and gray, carbon.

The dihedral angle between the central pyrrole and the adjacent outer pyrroles is 50°. The N(pyrrole)···O(ester) distance observed in the solid state is 2.999 Å and the N(pyrrole)—H···O(ester) angle is 145°, findings that are consistent with the hydrogen bonds in the self-assembled form of **24** being relatively weak.

4.3.4. Hexapyrrin

Another interesting solid state structure is observed in the case of hexapyrrin (**25**) [49]. Although this free base system possesses a fully conjugated electronic structure and an exocyclic double bond that is present in the *Z* configuration, in the solid state compound **25** is not completely planar. Presumably as a consequence, it exists in the form of a hydrogen-bonded network.

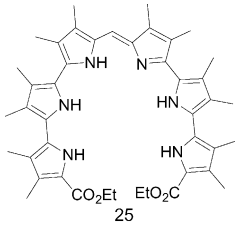

25

In analogy to what was seen in the case of the terpyrrole structure discussed above, large dihedral angles are observed between adjacent bipyrrolic pyrroles (the torsion angles for N1—C7—C8—N2 and N2—C11—C12—N3 are 120.5(7)° and −49.3(9)°, respectively), whilst the four other pyrrole units are nearly coplanar (Fig. 21). Short hydrogen bonds are observed between N3H and N4 (N3—N4 distance = 2.738 Å) that presumably add additional rigidity to the conjugated dipyrromethane subunit, while providing a sub-structure that bears analogy to the hair pin turns that serve to stabilize protein β-sheets.

The overall network produced by **25** is held together in the solid state by two N(pyrrole)—O(ester) H-bonds with an N(pyrrole)—O(ester) distance of 2.807(8) Å and an N1—H···O2 angle of 171.2(6)°. These hydrogen bond dimers are then further hydrogen bonded to adjacent dimers by one N2(pyrrole)—O3(ester) H-bond (N3—O2 distance = 2.992 5(7) Å; N3—H···O angle = 156···1(6)°) in a repeating fashion that results in layers of H-bound molecules.

4.3.5. Bicyclic pyrroles

Uno et al. [50] recently synthesized a series of pyrroles fused to a rigid bicyclic ring system via the pyrrolic β-positions. The systems that pertain to our discussion are the [2,2,1]bicylic derivative **26** and the [2,2,2]bicyclic derivative **27**. These compounds can exist in *syn* or *anti* forms, depending on whether the ester functions are found on the same or opposite sides of the bicyclic ring.

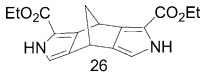

26

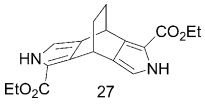

27

In the solid state (cf. Figs. 22 and 23), systems **26** and **27** are found to self-assemble in a very ordered fashion to generate structures that bear some resemblance to the arrays obtained with the various pyrrole ferrocene derivatives described previously (cf. Figs. 7 and 8). The self-assembly of systems **26** and **27** can be considered classic in that it operates through the mode represented by Structure **I** in Scheme 1. Nonetheless, these structures reveal fascinating features, in particular the fact that the overall solid state supramolecular arrangement is completely different in the case of the [2,2,1]bicyclic derivative **26** as compared to the [2,2,2]bicyclic derivative **27**.

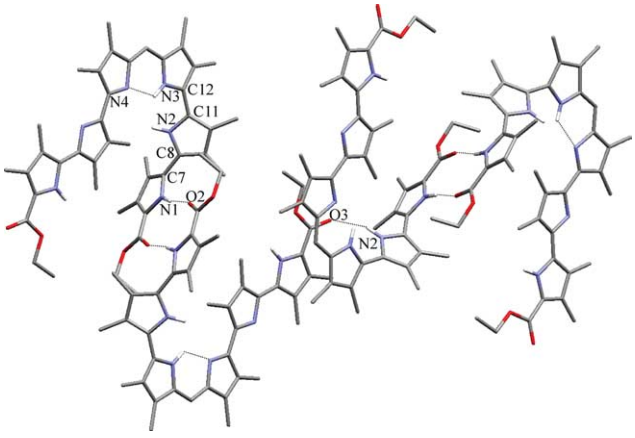

Fig. 21. X-ray structure of hexapyrrin (**25**) showing key noncovalent interactions. The overall supramolecular structure consists of layers of hydrogen bound molecules. This figure was generated using information downloaded from the Cambridge Crystallographic Data Centre and corresponds to a structure reported in [49]. Atom color codes in: red, oxygen; blue, nitrogen; and gray, carbon.

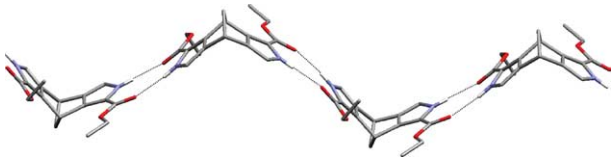

Fig. 22. X-ray structure of **26** showing the supramolecular ribbons present in the solid state form of this [2,2,1]bicyclic derivative. This figure was generated using information downloaded from the Cambridge Crystallographic Data Centre and corresponds to a structure reported in [50]. Atom color codes in: red, oxygen; blue, nitrogen; and gray, carbon.

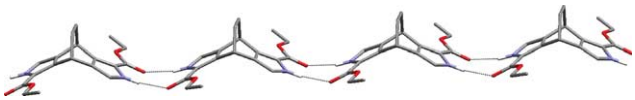

Fig. 23. X-ray structure of **27** showing the supramolecular ribbons present in the solid state of this [2,2,2]bicyclic derivative. This figure was generated using information downloaded from the Cambridge Crystallographic Data Centre and corresponds to a structure reported in [50]. Atom color codes in: red, oxygen; blue, nitrogen; and gray, carbon.

In the case of **26**, all the bicyclic rings are oriented in the same direction, whereas in **27**, they are arranged in an alternate manner. In both compounds, the individual bicyclic subunits are concave, with angles of 125° and 110° between the individual two pyrrolic units being seen in the case of **26** and **27**, respectively.

In terms of specifics, the hydrogen bonded assembly formed from **26** is of the classic type as illustrated in schematic form by Structure **VI** in Scheme 6. The hydrogen bonds are within typical values, with the average N···O distance being 2.87 Å and the average N—H···O angle being 167°. The hydrogen bond geometry observed in **27** (N···O distance of 2.871 Å and a N—H···O angle of 168°) is almost identical to that of **26**.

It appears likely that the different orientation of the two bicyclic rings observed in the solid state structures is largely due to the differing angles between the two concave pyrrolic subunits, with the wider pyrrole plane-to-pyrrole plane angle observed in **27** allowing for the formation of a stable H-bonded network without requiring the [2,2,2]bicyclic system to undergo a significant change in orientation.

4.3.6. Trisimine tripod

Over the past few years, Anslyn and co-workers [51–54] have introduced triply functionalized hexakis substituted benzene "pinwheels" as versatile preorganized, C_3 symmetric scaffolds for the generation of molecular receptors. In collaboration with Sessler et al., Anslyn et al. have recently begun exploring the use of this kind of scaffold to generate novel polypyrrolic entities. One of the first offshoots of this ongoing research effort is compound **28** (Fig. 24). This compound is unique among the self-assembled systems studied to date in that it contains imines as a key part of the covalent structure. Although sensitive to hydrolysis, the imine functionality provides a very basic nitrogen atom, a feature that makes it a potentially potent hydrogen-bond acceptor.

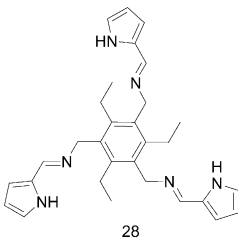

28

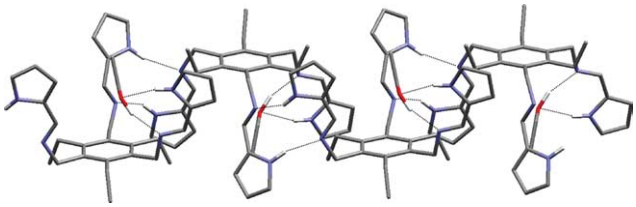

Fig. 24. X-ray structure of **28** illustrating the infinite assembly present in the solid state. Atom color codes in: red, oxygen; blue, nitrogen; and gray, carbon.

Single crystal X-ray diffraction analysis of **28** reveals that it does indeed undergo hydrogen bond-mediated self-assembly in the solid state. The resulting ensemble consists of a hydrogen bonded network of "trisimine pinwheel" subunits wherein one arm of the pinwheel binds another arm in the so-called "classic" fashion (cf. Structure **I** in Scheme 1). To accommodate the rigid framework defined by the "pinwheel" scaffold, the two complementary arms are twisted towards one another. This is reflected in quantitative terms by an observed N3—N4—N5—N6 torsion angle of 33.9°. The average N(pyrrole)···N(imine) distance is 2.9(16) Å. Again, the average N(pyrrole)—H···N(imine) hydrogen bond angle of a 154° is severely distorted from linearity because of this twisting of the arms. The third arm is not directly involved in inter- or intrasubunit interactions but, rather, is bound to an ethanol molecule via two hydrogen bonds.

4.3.7. Natural products

Pyrroles are ubiquitous in the biosphere and represent the key subunits in porphyrins, chlorines, B_{12} and a range of other macrocyclic products. Pyrroles are also found in metal-free form in numerous other naturally occurring compounds. Several of these latter species, as well as precursors and analogues, have been synthesized and characterized by X-ray diffraction studies. However, to date the resulting structures have rarely been considered from the perspective of whether or not the species in question self-assemble in the solid state. On the other hand, as discussed more fully below, a reexamination of these solid state structures reveals at least one unique, pyrrole-based supramolecular binding mode, as well as a range of more common self-assembled motifs.

One compound that highlights particularly interesting binding motifs is the di-arylated pyrrole (**29**) [55], a configurationally stable structural analogue of the powerful antimiotic agent, combrestastatin A-4 (Fig. 25) [56].

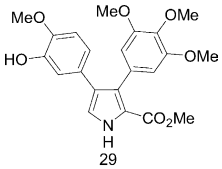

29

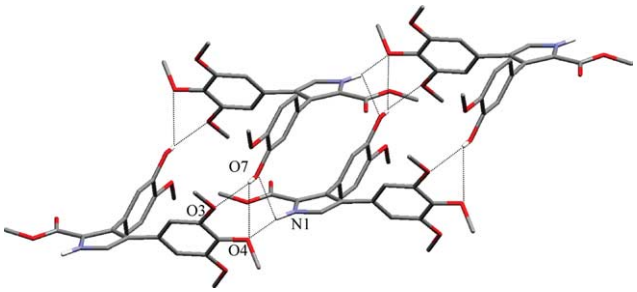

Fig. 25. X-ray structure of **29** showing the complex H-bonded array present in the solid state. This figure was generated using information downloaded from the Cambridge Crystallographic Data Centre and corresponds to a structure reported in [55]. Atom color codes in: red, oxygen; blue, nitrogen; and gray, carbon.

In the case of **29**, a particularly high density of hydrogen bond acceptor and donor functionality allows for the stabilization of a complex solid state self-associated network. In the single crystal X-ray structure of **29**, a unique example of a bifurcated hydrogen bond between the pyrrolic NH and two different phenolic oxygen acceptors is observed. It is characterized by an N1···O4 distance of 2.996 Å and an N1···O7 distance of 3.006 Å. The phenol moiety participates in three hydrogen bonds involving the pyrrolic NH and two methoxy substituents. For these interactions, the O7···O4 and O7···O3 bond distances are 2.938 and 2.799 Å, respectively. Interestingly, the oxygen atoms of the ester functionality are not playing an apparent role within the hydrogen bonded network, as is usually observed (cf. Structures **7**, **8**, and **9** in Section 4.2.2).

Other structures solved in the course of work devoted to natural product synthesis include those of **30**, **31**, and **32** [57–59]. In all cases, normal, or classic self-assembled motifs are seen in the solid state.

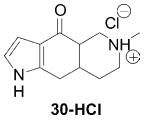

30-HCl

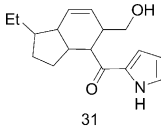

31

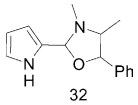

32

These simple examples bring up the question of the supramolecular role, if any, played by pyrrole-based metabolites in natural systems. Does Nature use hydrogen donating ability of pyrroles to her advantage and, if so, how? Currently, there is very little in the way of real information that touches on this matter, particularly as regard the organized pyrrole–pyrrole interactions analogous to those discussed in this review. However, it has been proposed that prodigiosin mediates its biological activity through uncoupling of proton translocators as the result of effecting the cotransport of protons and chloride anions across biological membranes [60,61]. Dipyrrolyl intermediates present along the biosynthetic pathway leading to heme may also act to bind the carboxylate side chain of a key aspartic acid residue [62].

4.4. Octafluorocalix[4]pyrrole

In a quest to generate analogues of calix[4]pyrrole displaying higher binding affinities, Sessler et al. [63] synthesized a perfluorinated analogue **33**. This analogue not only showed a dramatic increase in affinity toward both neutral and anionic substrates, it also was found to exist in the form of a self-assembled trimer in the solid state (Fig. 26).

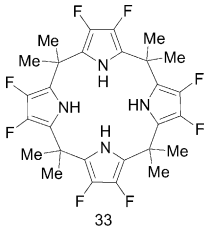

33

The aggregated form of **33** consists of a 1:1 mixture of monomers in the so-called 1,2-alternate and 1,3-alternate conformations. The existence of these two conformations is to be contrasted with the cone conformation observed in dimer, **2**·**2** (vide supra) and allows the formation of a trimer wherein the fluoro substituents in the 3 and 4 position act as hydrogen bond acceptors. The resulting binding motif is of the general type

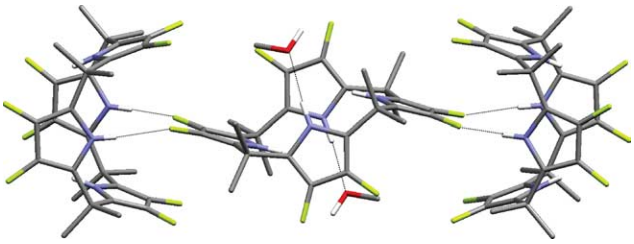

Fig. 26. X-ray structure of the hydrogen bonded trimer found in crystals of calix[4]fluoropyrrole (**33**). This figure was generated using information downloaded from the Cambridge Crystallographic Data Centre and corresponds to a structure reported in [63]. Atom color codes in: blue, nitrogen; gray, carbon; and green, fluoride.

represented by Structure **IV** of Scheme 4. However, it is important to note that in both monomeric conformers, only two out of the four pyrrole subunits are involved in hydrogen bonding; the other two remain as spectators. Interestingly, the Nature of the hydrogen bond participation varies, with the central calix[4]pyrrole (present in its 1,2-alternate conformation) acting only as a hydrogen bond acceptor through the beta pyrrolic fluorine substituents, whilst the two adjacent calix[4]pyrroles, both present in the trimer in their respective 1,3-alternate conformations, act as hydrogen bond donors through two (out of four) of their pyrrolic NH protons. The average NH···F distance is 2.969 Å and the average N—H···F angle is 171°.

4.5. Hybrid heterocalixarenes

Recently, Sessler et al. [64] have prepared several novel hybrid heterocalixarenes that could serve as possible building blocks for the construction of self-assembled systems. Although the development of this chemistry remains in its infancy, several interesting ensembles have already been characterized as the result of X-ray diffraction analysis. One example is provided by the symmetric heterocalixarene, calix[2]benzene[2]pyrrole (**34**), which provides a specific embodiment of the generalized Structure **V** shown in Scheme 5.

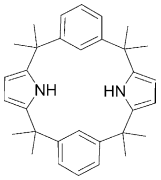

34

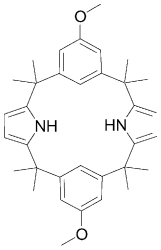

35

In the solid state, compound **34** exists in the form of a dimer, with this dimer being stabilized as the result of a molecule of dimethoxyethane which acts as a double H-bond acceptor (Fig. 27). The geometry of the various stabilizing interactions is: N1—H1···O2, N···O 3.042(2) Å, H···O 2.11(2) Å, N—H···O 175(2)°. The individual phenyl and pyrrole rings are oriented in what is perhaps best described as a 1,3-alternate conformation. Specifically, the protons on the 2-position of the benzene

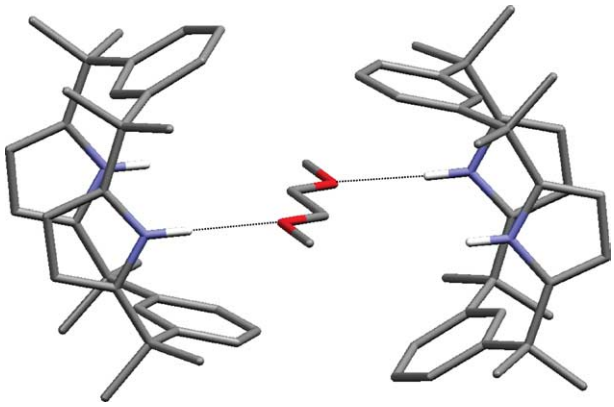

Fig. 27. X-ray structure of the calix[2]benzene[2]-pyrrole (**34**) showing dimethoxyethane-mediated self-assembled motifs present in the solid state. This figure was generated using information downloaded from the Cambridge Crystallographic Data Centre and corresponds to a structure reported in [64]. Atom color codes in: red, oxygen; blue, nitrogen; and gray, carbon.

subunits point away from the NH protons present in the two "center" pyrrolic rings.

The *trans*-calix[2]-5-methoxybenzene[2]pyrrole (**35**) differs from **34** in that it bears two methoxy substituents. As such, it contains built-in hydrogen-bond donor and acceptor functionality. Presumably, as a consequence of this duality, it exists as an offset dimer in the solid state. Here, as illustrated in Fig. 28, the two individual macrocyclic subunits are linked through two hydrogen-bonding interactions that involve collectively the 5-methoxybenzene oxygen atoms and the pyrrole NH protons. However, the hydrogen bonding interactions are presumably very weak as reflected in the long N···O distance of 3.319(3) Å and the rather distorted N—H···O angle of 146(1)°.

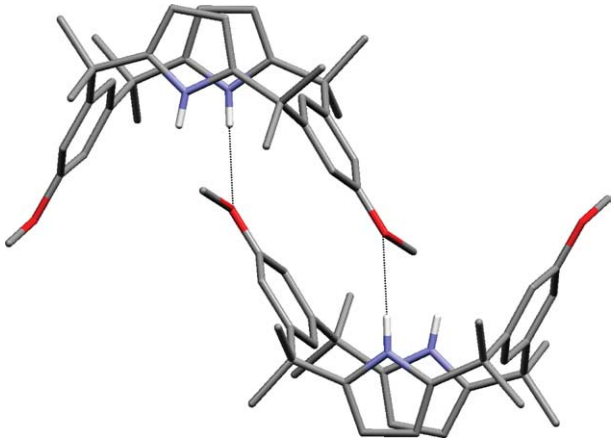

Fig. 28. View of the hydrogen bonded dimer observed in crystals of **35**. This figure was generated using information downloaded from the Cambridge Crystallographic Data Centre and corresponds to a structure reported in [64]. Atom color codes in: red, oxygen; blue, nitrogen; and gray, carbon.

4.6. Dipyrrolylquinoxaline-derived ensembles

Dipyrrolylquinoxaline derivatives have emerged as a new class of easy-to-make anion receptors [63,65–67]. As a class, they have proved particularly sensitive to fluoride anion, a substrate that engenders a strong colorimetric response. These molecules contain both, hydrogen bond donors (pyrroles) and acceptors (quinoxaline nitrogens). As in other systems containing built in donors and acceptors, this duality enables dipyrrolylquinoxaline, such as **36**, to form hydrogen bonded networks in the solid state as revealed by X-ray diffraction analysis (Fig. 29).

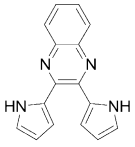

36

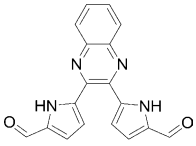

37

Interestingly, only one of the two pyrrolic subunits was found to be involved in the requisite intermolecular hydrogen bonding interactions. This particular pyrrole tilts away from the plane formed by the quinoxaline scaffold by roughly 90° (the dihedral angle defined by N1—C2—C6—N7 is 89.9(2)°), whereas the other pyrrole remains in the same plane as the quinoxaline (the relevant dihedral angle, defined by N17—C16—C15—N14, is −1.7(3)°). The geometry of the pyrrole NH-to-quinoxaline hydrogen bond is within the expected values, with the N(pyrrole)···N(quinoxaline) and N(pyrrole)H···N(quinoxaline) distances being 3.0539(2) and 2.07(3) Å, respectively. The N(pyrrole)—H···N(quinoxaline) angle is 179(2)°. This value, which is very close to linear, is noteworthy in the context of the other structures stabilized by pyrrole-containing subunits.

In the case of the 2,2′-diformylpyrrole substituted quinoxaline (**37**), the so-called classic binding mode, involving interactions between the pyrrolic NH and an adjacent aldehyde carbonyl, is observed in the solid state. This leads to the formation of a supramolecular ribbon (Fig. 30), a type of association specifically shown as Structure **VI** of Scheme 6. In the context of forming such a network, the two pyrrole moieties tilt away from the quinoxaline plane in a symmetrical fashion to produce a C_2 symmetric structure. The torsion angle between the central quinoxaline and the plane defined by a neighboring pyrrole is 26.66(15)°. The quinoxaline subunit is itself somewhat ruffled with the dihedral angle defined by C6—C6′—C8—C8′ being 8.14(19)°.

All the hydrogen bonds present in the network produced by the solid state self-assembly of **37** are identical, with the N(pyrrole)···O(aldehyde) and N(pyrrole)H···O(aldehyde) distances being 2.848(12) and 1.954(16) Å, respectively. The N(pyrrole)H···O(aldehyde) angle is 168.6(13)°.

The ''crowned'' dipyrrolylquinoxaline derivative **38** forms a unique tetramer in the solid state, presumably because of the steric bulk associated with the 18-crown-6 moiety [68]. This tetramer can be viewed as a potential channel for small entities such as water molecules or anions.

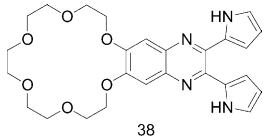

38

The supramolecular motif highlighted in Fig. 31 is reinforced by numerous hydrogen bonds, all of which occur in a regular pattern. For instance, when looking at the top face of the tetramer unit, it can be seen that there are two molecules on opposite corners of the ''square'' that have their quinoxaline unit overlaying the quinoxaline unit on the molecule adjacent to it. Only the inward facing pyrrole NH atoms (N1A and N1B) of the two overlaying molecules participate in hydrogen bonding to the encapsulated water molecule (NH···Ow of 2.13 Å). Likewise, it is also only the overlaying, inward facing pyrazine nitrogens (N3A and N3B) that participate in hydrogen bonding to this same molecule

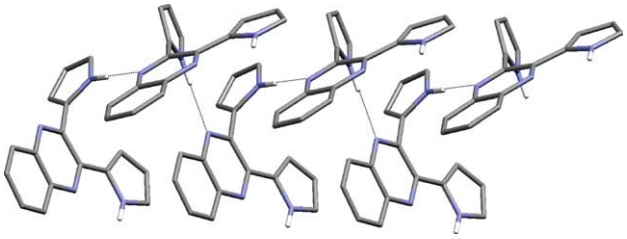

Fig. 29. View of the hydrogen bonded network observed in crystals of dipyrrolylquinoxaline (**36**). Atom color codes in: blue, nitrogen; and gray, carbon.

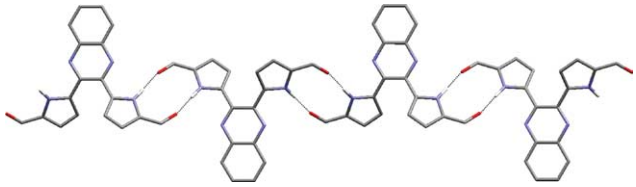

Fig. 30. Solid state structure of the hydrogen bonded ribbon formed by the self-assembly of **37**. Atom color codes in: red, oxygen; blue, nitrogen; and gray, carbon.

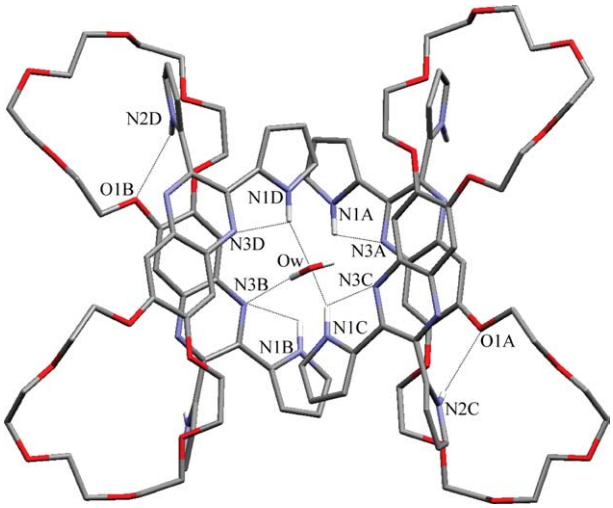

Fig. 31. X-ray structure of the supramolecular tetramer that exists as a repeating motif in crystals of **38**. This figure was generated using information downloaded from the Cambridge Crystallographic Data Centre and corresponds to a structure reported in [68]. Atom color codes in: red, oxygen; blue, nitrogen; and gray, carbon.

of water (N···H—Ow of 2.08 Å). Intramolecular hydrogen bonding interactions are present between the inward-pointing pyrazine nitrogen atoms of all four quinoxalines in the tetramer and the inward pointing pyrrole NH atoms, specifically N3A to N1A, N3B to N1B, N3C to N1C, and N3D to N1D; N···HN of 2.49 Å.

Curiously, the only direct interactions between the two "layers" seen in this view (Fig. 32) are hydrogen bonds between one of the methoxy-like oxygens in the phenolic position of the overlaying quinoxaline and the NH of the outward-facing pyrrole of the corresponding underlying unit (O1A to N2C and O1B to N2D; NH···O of 2.20 Å). This extraordinary ensemble is thus stabilized by 10 hydrogen bonds: two NH···Ow, two N···H—Ow, four N···HN, and two NH···O interactions.

The supramolecular channel-like motif produced by **38** in the solid state can be destroyed by the addition of potassium cation, a species that, because of its size, induces dimerization of the crown components (and hence the molecule as a whole) in the solid state (cf. Fig. 33).

The "crowned"-dipyrrolylquinoxaline derivative **38** forms a 2:1, ligand:K^+ intermolecular complex with the benzo-15-crown-5 unit from each dipyrrolylquinoxaline sandwiching the potassium cation. The K···O distances range from 2.795(2) to 2.995(2) Å. The formation of such a sandwich complex is not uncommon and the distances are well within the normal limits for such contacts [69–73]. As a result of these interactions, the two sets of bifurcated hydrogen bonds between N2···O4′ and N2···O5′ seen in Fig. 31 for the free receptor are no longer present. Presumably as a consequence, molecules of the 'crowned'-quinoxaline are offset from one another, giving what is presumably the lowest energy, least sterically hindered structure.

The dimethoxy quinoxaline derivative **39**, which represents a close electronic analogue to the crown quinoxaline described above, does not form a tetramer but simply dimerizes in the solid state (Fig. 34).

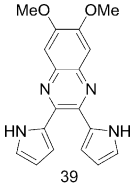

39

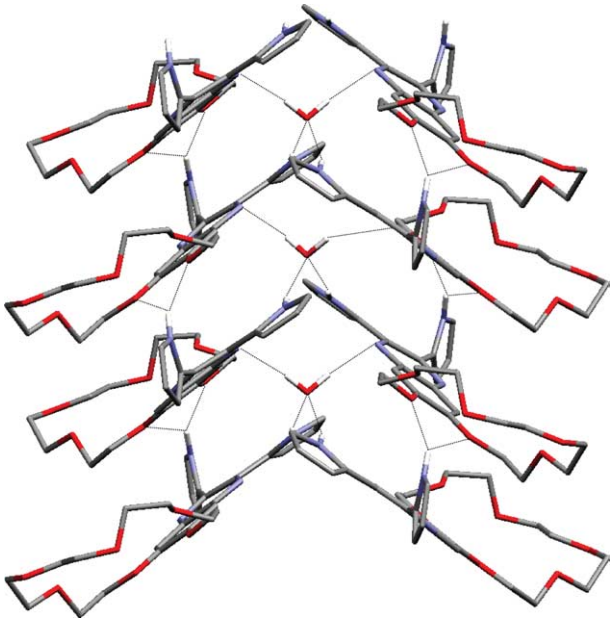

Fig. 32. Side-view of the X-ray structure of **38**. This figure was generated using information downloaded from the Cambridge Crystallographic Data Centre and corresponds to a structure reported in [68]. Atom color codes in: red, oxygen; blue, nitrogen; and gray, carbon.

This side view shows that **36** exists in an anti-parallel hydrogen-bound dimer, stabilized by two sets of identical intermolecular hydrogen-bonds from N4···O1′

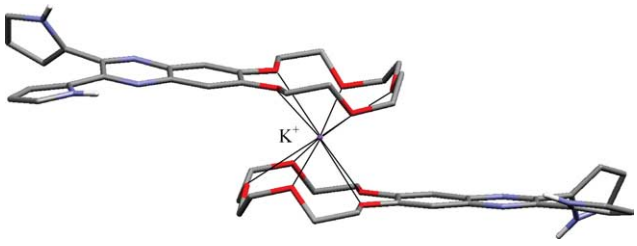

Fig. 33. Single X-ray structure showing the K^+ templated dimer formed from 18-crown-6-dipyrrolylquinoxaline (**38**). This figure was generated using information downloaded from the Cambridge Crystallographic Data Centre and corresponds to a structure reported in [68]. Atom color codes in: red, oxygen; blue, nitrogen; gray, carbon; and purple, potassium.

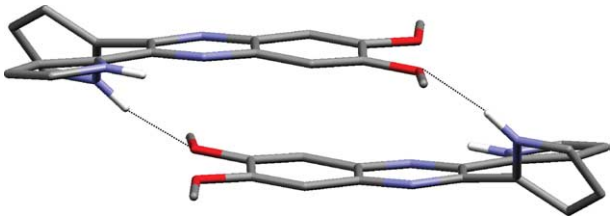

Fig. 34. X-ray structure of the dimethoxy dipyrrolylquinoxaline (**39**). Unlike the "crowned" quinoxaline (**38**), this system exists in the form of a dimer in the solid state. This figure was generated using information downloaded from the Cambridge Crystallographic Data Centre and corresponds to a structure reported in [68]. Atom color codes in: red, oxygen; blue, nitrogen; and gray, carbon.

(3.06 Å) and N4···O2′ (3.29 Å). In the unit cell, each dimer is further hydrogen-bound to an adjacent dimer, via a set of two pyrazine-N···pyrrole—NH interactions at a distance of 2.247 Å.

5. Concluding remarks

The examples assembled in this paper have served to illustrate that functionalized pyrroles represent powerful and useful precursors for the construction of solid state self-assembled ensembles. While a number of classic motifs, involving for the most part direct, usually dimeric interactions between pyrrole NH protons, acting as hydrogen bond donors, and appended carbonyl moieties, acting as hydrogen bond acceptors, have been identified, it is important to appreciate that a wide range of structural forms have already been characterized, including a full range of aesthetically pleasing, trimers, tetramers, ribbons, and tapes. The relevance of this work to natural product chemistry and the recognition that self-assemblies play a role in the world of biologically relevant molecules adds a special emphasis to this area of research and leads to the prediction that it will continue to evolve as an important sub-branch of molecular recognition chemistry.

6. Experimental

6.1. General remarks

Reagents were used as obtained from Aldrich Chemicals. ^{1}H and ^{13}C NMR spectra were recorded on a Brucker AC 250 spectrometer. Chemical shifts are reported relative to the deuterated solvents. IR spectra were recorded on a Mattson Genesis II FTIR spectrometer. Elemental analyses were performed by Atlantic Microlabs, Atlanta, GA, and are reported as percentages.

All NMR spectroscopic solvents were purchased from Cambridge Isotope Laboratories.

6.2. Synthesis of tris(2-(2-amidepyrrole)ethyl)amine (**20**)

Tris(2-aminoethyl)amine (283 mg, 1.9 mmol), 2-pyrrole carboxylic acid (640 mg, 5.8 mmol), and 1-hydroxybenzotriazole (HOBT) (783 mg, 5.8 mmol) were dissolved in DMF (50 ml) and stirred for 10 min., dicyclohexylcarbodimide (DCC) (1.435 g, 7 mmol) was then added and the mixture was stirred at room temperature for 24 h. The mixture was filtered, and the filtrate concentrated in vacuo, to give a yellow oil which was purified by column chromatography on neutral alumina (CH_2Cl_2/MeOH, 10:1). The resulting solid was subsequently recrystallized from methanol to yield white crystal (486 mg, 60%). M.p. 222–224 °C from methanol. IR (Teflon Card): $\tilde{\nu}$ = 3300–3100 (CON—H), 2850–2950 (C—H), 1620 (C=O) cm^{-1}. ^{1}H NMR (250 MHz, DMSO-d_6): $\delta = 2.65$ (t, $J = 6.7$ Hz, 6H, —CH_2—N), 3.29 (t, $J = 6.1$ Hz, 6H, CONH—CH_2—), 6.04 (d, $J = 2.98$ Hz, 3H, H_β), 6.71 (s, 3H, H_γ), 6.82 (s, 3H, H_α), 7.89 (t, $J = 6.1$ Hz, 3H, —CONH—), 11.39 (s, 3H, $N_{pyrrole}$—H) ppm. ^{13}C NMR (63 MHz, DMSO-d_6): 37.0 (CH2), 53.8 (CH2), 108.5 (CH), 109 (CH), 121.2 (C_q), 126.3 (C_q), 160.7 (C_q) ppm. MS (CI$^+$): m/z (%) = 427 [M$^{+\cdot}$] (21), 426 (100). High resolution MS (CI$^+$) for $C_{21}H_{27}N_7O_3$ requires MH 425.2254, found: 425.2259.

6.3. Synthesis of trisimine pinwheel (**28**)

1,3,5-Triethyl-2,4,6-tris(aminoethyl)benzene (Pinwheel, 100 mg, 0.4 mmol) and 2-pyrrole carboxaldehyde (115 mg, 1.2 mmol) were ground together in a 2 ml vial and heated for 20 s with a heat gun to give a solid melt. Compound **28** precipitated as a light yellow solid upon cooling. The product was directly recrystallized in the vial with 0.5 ml of absolute ethanol to give colorless crystals (155 mg, 80%). M.p. 203–204 °C (dec.) from ethanol. *Anal.* Calc. for **28** · **EtOH** $C_{32}H_{42}N_6$ O (526.24): C, 72.97; H, 8.04; N 15.96. Found: C, 72.94; H, 8.15; N, 15.94%. IR(Teflon Card): $\tilde{\nu}$ = 3100–3010 (C—H), 2962–2870 (C—H), 1628 (C=N) cm^{-1}. ^{1}H NMR (DMSO-d_6): $\delta = 1.05$ (t, 3H, EtOH), 1.16 (t, $J = 6.99$ Hz, 9 H, CH_3 Et), 2.73 (q, $J = 7.34$ Hz, 6H, CH_2 Et), 3.44 (q, 2H, EtOH), 4.71 (s, 6H, —CH_2—N=), 6.07 (s, 3H, H_β), 6.41 (s, 3H, H_γ), 6.81 (s, 3H, H_α), 8.11 (s, 3H, —HC=N—), 11.27 (s, 3H, NH) ppm. ^{13}C NMR (63 MHz, DMSO-d_6): 15.80 (Et), 18.58 (EtOH), 22,30 (Et), 56.07 (EtOH) 56.95 (—CH_2—), 108.88 ($C_{pyrrole}$-3), 113.49 ($C_{pyrrole}$-4), 122.15 ($C_{pyrrole}$-5), 130.08 ($C_{pyrrole}$-2), 132.89 (C-ar), 142.31 (C-ar), 151.38 (C=N) ppm. MS (CI$^+$): m/z (%) = 482 [M$^{+\cdot}$] (24.9), 481 (100).

6.4. Structure determination and refinement of **20**, **28**, **36**, and **37**

Crystals of **20** grew as large colorless prisms by slow evaporation from methanol solution; crystals of **28** grew

Table 1
X-ray crystallographic and experimental data for compounds **20**, **28**, **36**, and **37**

Receptor	**20**	**28**	**36**	**38**
Formula	$C_{21}H_{27}N_7O_3$	$C_{30}H_{36}N_6$—C_2H_5OH	$C_{16}H_{12}N_4$	$C_{18}H_{12}N_4O_2$
Formula weight (g mol_{-1})	425.50	526.72	260.30	316.32
Color, shape	colorless prisms	colorless prisms	yellow needle	yellow-green needle
Space group	$P-1$	$C_{2/c}$	$Pna2_1$	$C2/c$
a (Å)	10.1950(1)	21.9980(2)	6.8356(2)	9.4895(2)
b (Å)	10.4378(2)	4.1906(2)	19.2668(6)	15.0137(4)
c (Å)	10.9356(2)	20.9917(2)	9.5988(2)	10.6867(2)
α (°)	94.690(1)	$\alpha = 90$	90	90
β (°)	110.221(1)	$\beta = 114.729(1)$	90	102.532(1)
γ (°)	101.771(1)	$\gamma = 90$	90	90
V (Å^3)	1054.22(3)	5951.95(11)	1264.16(6)	1486.29(6)
Z	2	8	4	4
T (K)	153(2)	153(2	153(2)	153(2)
$D_{calc.}$ (g/cm^3)	1.340	1.176	1.368	1.414
μ (mm^{-1}) (Mo Kα)	0.094	0.073	0.085	0.096
λ (Å)	0.71073	0.71073	0.71073	0.71073
Crystal size (mm)	$0.30 \times 0.21 \times 0.14$	$0.31 \times 0.30 \times 0.27$	$0.30 \times 0.10 \times 0.10$	$0.40 \times 0.15 \times 0.15$
$R_w(F^2)$[a]	0.0342	0.0428	0.0406	0.0363
$R(F)$ $[I > 2\sigma(I)]$[b]	0.0836	0.00994	0.0925	0.0986
Goodness-of-fit on F^2[c]	1.003	1.009	1.027	1.063
Number of total, unique reflections	7771, 4786	12 731, 6807	2681, 2681	3083, 1692
Number of parameters, restraints	389, 0	369, 0	230, 0	134, 0

[a] $R_w(F^2) = \{\Sigma_w(|F_o|^2 - |F_c|^2)^2/\Sigma_w(|F_o|)^4\}^{1/2}$, where w is the weight given for each reflection.
[b] $R(F) = \Sigma(|F_o| - |F_c|)/\Sigma|F_o|\}$ for reflections with $F_o > 4(\sigma(F_o))$.
[c] $S = [\Sigma_w(|F_o|^2 - |F_c|^2)^2/(n-p)]^{1/2}$, where n is the number of reflections and p is the number of refined parameters.

as large colorless prisms by slow evaporation from absolute ethanol solution; Crystals of **36** grew as yellow needles by slow evaporation from CH_2Cl_2 solution; and crystals of **37** grew as yellow-green needles by slow evaporation from hexanes–CH_2Cl_2 solution.

The data were collected on a Nonius Kappa CCD (Mo Kα radiation). Data reduction were performed using DENZO-SMN [74]. The structure was solved by direct methods (SIR92 [75]) and refined by full-matrix least-squares on F^2 with anisotropic displacement parameters for the non-H atoms (SHELXL-97 [76]). The hydrogen atoms were located in a ΔF map and refined with isotropic displacement parameters. Definitions used for calculating $R(F)$, $R_w(F_2)$ and the goodness of fit, S, are given below. The data were corrected for secondary extinction effects. Relevant crystals and data parameters are presented in Table 1. Graphical illustrations were performed with MERCURY software.

7. Supporting information

CCDC 188997, 188217, 188263, and 188265 contain the supplementary crystallographic data for structures **20**, **28**, **36**, and **37**, respectively. These data can be obtained free of charge at www.ccdc.cam.ac.uk/conts/retrieving.html [or from the Cambridge Crystallographic Data Centre, 12 Union Road, Cambridge CB2 1EZ, UK; fax: (internat.) +44-1223/336-033; E-mail: deposit@ccdc.cam.ac.uk].

Acknowledgements

This work was supported in part by grants from the R.A. Welch Foundation (Grant Nos. F-1151 and F-1018 to E.V.A and J.L.S), the Department of Energy (Grant No. DE-F003 – 01ER-15186 jointly to J.L.S. and E.V.A.), the National Institutes of Health (Grant No. 58907 to J.L.S.), the National Science Foundation (Grant No. CHE-0107732 to J.L.S.), the Royal Society (University Research Fellowship to P.A.G.), and EPSRC (fast stream studentship grant to P.A.G.). Support for H.M. came from a JSPS Research Fellowship for Young Scientists; he thanks Prof. Atsuhiro Osuka (Kyoto University) for a study leave.

References

[1] J.L. Atwood, J.E.D. Davies, D.D. MacNicol, F. Vogtle, Comprehensive Supramolecular Chemistry, Elsevier, Oxford, 1996.
[2] J.-M. Lehn, Supramolecular Chemistry, VCH, Weinheim, 1995.
[3] D.S. Lawrence, T. Jiang, M. Levett, Chem. Rev. 95 (1995) 2229.
[4] D. Philip, J.F. Stoddart, Angew. Chem., Int. Ed. Engl. 35 (1996) 1154.
[5] F. Vogtle, Supramolecular Chemistry, Wiley, Chichester, 1991.
[6] G.M. Whitesides, E.E. Simanek, J.P. Mathias, C.T. Seto, D.N. Chin, M. Mammen, D.M. Gordon, Acc. Chem. Res. 28 (1995) 37.
[7] J.S. Lindsey, New J. Chem. 15 (1991) 153.
[8] J.R. Rebek Jr., Angew. Chem., Int. Ed. Engl. 29 (1990) 245.
[9] C.A. Hunter, Angew. Chem., Int. Ed. Engl. 34 (1995) 1079.
[10] J.C. MacDonald, G.M. Whitesides, Chem. Rev. 9 (1994) 2383.

[11] D. Voet, J.G. Voet, Biochemistry, second ed., Wiley, New York, 1995.
[12] C. Branden, J. Tooze, Introduction to Protein Structure, Garland, New York, 1991.
[13] A. Fersht, Enzyme Structure and Mechanism, second ed., Freeman, New York, 1984.
[14] J.L. Sessler, A. Andrievsky, P.A. Gale, V. Lynch, Angew. Chem., Int. Ed. Engl. 35 (1996) 2782.
[15] P.A. Gale, S. Camiolo, M.B. Hursthouse, M.E. Light, A.J. Shi, Chem. Commun. (2002) 758.
[16] P.A. Gale, G. Denault, M.B. Hursthouse, M.E. Light, C.N. Warriner, New J. Chem. (2002) 812.
[17] P.A. Gale, S. Camiolo, M.E. Light, C.P. Chapman, M.E. Light, M.B. Hursthouse, Tetrahedron Lett. 42 (2001) 5095.
[18] P.A. Gale, S. Camiolo, J.G. Tizzard, C.P. Chapman, M.E. Light, S.J. Coles, M.B. Hursthouse, J. Org. Chem. 66 (2001) 7849.
[19] M. Shionoya, H. Furuta, V. Lynch, A. Harriman, J.L. Sessler, J. Am. Chem. Soc. 114 (1992) 5714.
[20] P.A. Gale, J.L. Sessler, V. Kral, V. Lynch, J. Am. Chem. Soc. 118 (1996) 5140.
[21] C. Schmuck, Eur. J. Org. Chem. (1999) 2397.
[22] C. Schmuck, J. Lex, Org. Lett. 1 (1999) 1779.
[23] C. Schmuck, J. Lex, Eur. J. Org. Chem. (2001).
[24] A. Bianchi, K. Bowman-James, E.G. Espana, Supramolecular Chemistry of Anions, Wiley-VCH, New York, 1997.
[25] G. Muller, J. Reide, F.P. Schmidtchen, Angew. Chem., Int. Ed. Engl. 27 (1988) 1516.
[26] J.L. Sessler, A. Andrievsky, F. Ahuis, F. Vogtle, D. Gudat, M. Moini, J. Am. Chem. Soc. 120 (1998) 9712.
[27] J.L. Sessler, M. Scherer, A. Gebauer, V. Lynch, Chem. Commun. (1998) 85.
[28] J. Gokel, C. Li, J.C. Medina, G.E. Maguire, E. Abel, J.L. Atwood, J. Am. Chem. Soc. 119 (1997) 1609.
[29] J.L. Sessler, M. Moini, M. Scherer, A. Gebauer, V.M. Lynch, Chem. Eur. J. 4 (1998) 152.
[30] M. Scherer, J.L. Sessler, A. Gebauer, V. Lynch, J. Org. Chem. 6 (1997) 7877.
[31] R.H. Crabtree, K. Kavallieratos, S.R.d. Gala, D.J. Austin, J. Am. Chem. Soc. 119 (1997) 2325.
[32] R. Bonnet, M.B. Hursthouse, S. Niedle, J. Chem. Soc., Perkin Trans. 2 (1972) 13335.
[33] P.A. Gale, K. Navakhun, S. Camiolo, M.E. Light, M.B. Hursthouse, Chem. Commun. (2002) 2084.
[34] S. Camiolo, S.J. Coles, P.A. Gale, M.B. Hursthouse, G.J. Tizzard, Supramolecular Chem. 15 (2003) 231.
[35] S. Camiolo, P.A. Gale, M.B. Hursthouse, M.E. Light, Org. Biomol. Chem. 1 (2003) 741.
[36] S. Camiolo, P.A. Gale, M.B. Hursthouse, M.E. Light, A.J. Shi, Chem. Commun. (2002) 758.
[37] J. Sanxhez-Quesada, C. Seel, P. Prados, J.d. Mendoza, J. Am. Chem. Soc. 118 (1996) 277.
[38] M.C.T. Fyfe, P.T. Glink, S. Menzer, J.F. Stoddart, A.J.P. White, D.J. Williams, Angew. Chem., Int. Ed. Engl. 36 (1997) 2068.
[39] G.M. Hubner, J. Glaser, C. Seel, F. Vogtle, Chem. Eur. J. 38 (1999) 383.
[40] B. Hasenknopf, J.-M. Lehn, N. Boumediene, A. Dupont-Gervais, A.v. Dorsselar, B.O. Kniesel, A. Fersht, J. Am. Chem. Soc. 119 (1997) 10956.
[41] B. Hasenknopf, J.-M. Lehn, B.O. Kniesel, G. Baum, D. Fenske, Angew. Chem., Int. Ed. Engl. 35 (1996) 1838.
[42] J.A. Wisner, P.D. Beer, M.G.B. Drew, Angew. Chem., Int. Ed. Engl. 40 (2001) 3606.
[43] P.A. Gale, K. Navakhun, S. Camiolo, M.E. Light, M.B. Hursthouse, J. Am. Chem. Soc. 124 (2002) 11228.
[44] J.L. Sessler, G. Kirkovits (2002) Unpublished work.
[45] A. Merz, J. Kronberger, L. Dunsch, A. Neudeck, A. Petr, L. Parkanyi, Angew. Chem., Int. Ed. Engl. 38 (1999) 1442.
[46] J.L. Sessler, W.E. Allen, C.J. Fowler, V.M. Lynch, Chem. Eur. J. 7 (2001) 721.
[47] J.L. Sessler, M.C. Hoehner, D.W. Johnson, A. Gebauer, V. Lynch, Chem. Commun. 20 (1996) 2311.
[48] J.L. Sessler, S.J. Weghorn, Y. Hiseada, V. Lynch, Chem. Eur. J. 1 (1995) 56.
[49] J.L. Sessler, P. Morosini, M. Shere, S. Meyer, V. Lynch, J. Org. Chem. 62 (1997) 8848.
[50] H. Uno, S. Ito, M. Wada, H. Watanabe, M. Nagai, A. Hayashi, T. Murashima, N. Ono, J. Chem. Soc., Perkin Trans. 1 (2000) 4347.
[51] A. Metzger, V.M. Lynch, E.V. Anslyn, Angew. Chem., Int. Ed. Engl. 36 (1997) 862.
[52] J.J. Lavigne, S. Savoy, M.B. Clevenger, J.E. Ritchie, B. McDoniel, S.J. Yoo, E.V. Anslyn, J.T. McDevitt, J.B. Shear, D. Neikirk, J. Am. Chem. Soc. 120 (1998) 6429.
[53] G. Hennrich, E.V. Anslyn, Chem. Eur. J. 8 (2002) 2219.
[54] S.L. Wiskur, H. Ait-Haddou, J.J. Lavigne, E.V. Anslyn, Acc. Chem. Res. 34 (2001) 963.
[55] M.G. Banwell, B.L. Flynn, E. Hamel, D.C.R. Hockless, Chem. Commun. (1997) 207.
[56] R.T. Brown, B.W. Fox, J.A. Hadfield, A.T. McGown, S.P. Mayalarp, G.R. Pettit, J.A. Woods, J. Chem. Soc., Perkin Trans. 1 (1995) 577, and references cited therein.
[57] G.L. Olson, H.-C. Cheung, K.D. Morgan, J.F. Blount, L. Todaro, L. Berger, J. Med. Chem. 24 (1981) 1026.
[58] M.P. Edwards, S.V. Ley, S.G. Lister, B.D. Palmer, D.J. Williams, J. Org. Chem. 49 (1984) 3503.
[59] J.F. Gallagher, L.M. Fitzsimons, Acta Crystallogr., Sect. C C55 (1999) 1000.
[60] S. Ohkuma, T. Sato, M. Okomato, H. Matsuya, K. Arai, T. Kataoka, Biochem. J. 334 (1998) 731.
[61] T. Sato, H. Konno, Y. Tanaka, T. Kataoka, K. Nagai, H.H. Wasserman, S. Ohkuma, J. Biol. Chem. 273 (1998) 21455.
[62] P.M. Jordan, Curr. Opin. Struct. Biol. 4 (1994) 902.
[63] J.L. Sessler, P. Anzenbacher Jr., K. Jursikova, A.C. Try, H. Miyaji, V. Lynch, M. Marquez, J. Am. Chem. Soc. 122 (2000) 10268.
[64] J.L. Sessler, W.-S. Cho, V. Lynch, V. Kral, Chem. Eur. J. 8 (2002) 1134.
[65] J.L. Sessler, C.B. Black, B. Andrioletti, A.C. Try, C. Ruiperez, J. Am. Chem. Soc. 121 (1999) 1438.
[66] J.L. Sessler, T. Mizuno, W.H. Wei, L.R. Eller, J. Am. Chem. Soc. 124 (2002) 1134.
[67] J.L. Sessler, M. Hiromistu, T. Mizuno, V. Lynch, H. Furuta, Chem. Commun. (2002) 862.
[68] G.J. Kirkovits, R.S. Zimmerman, M.T. Huggins, V. Lynch, J.L. Sessler, Eur. J. Org. Chem. (2002) 3768.
[69] P.R. Mallinson, M.R. Truter, J. Chem. Soc., Perkin Trans. 2 (1972) 1818.
[70] T.N.S. Shinkai, T. Ogawa, K. Shigematsu, O. Manabe, J. Am. Chem. Soc. (1981) 111.
[71] K. Kikukawa, G.-X. He, A. Abe, R.A.T. Goto, T. Ikeda, F. Wada, T. Matsuda, J. Chem. Soc., Perkin Trans. 2 (1987) 135.
[72] P.D. Beer, E.L. Tite, A.J. Ibbotson, J. Chem. Soc., Dalton Trans. (1990) 2691.
[73] P.D. Beer, M.G.B. Drew, R.J. Knubley, M.I. Ogden, J. Chem. Soc., Dalton Trans. (1995) 3117.
[74] Z. Otwinowski, W. Minor, Methods Enzymol. 276 (1997) 276.
[75] A. Altomare, G. Cascarano, C. Giacovazzo, A. Guagliardi, J. Appl. Cryst. 26 (1993) 343.
[76] G.M. Sheldrick, SHELXL-97. Program for the Refinement of Crystal Structures, University of Gottingen, Germany, 1997.